SIAM J. APPL. MATH.
Vol. 57, No. 4, pp. 1044–1081, August 1997

009

AGGREGATION, BLOWUP, AND COLLAPSE: THE ABC'S OF TAXIS IN REINFORCED RANDOM WALKS*

HANS G. OTHMER† AND ANGELA STEVENS‡

Abstract. In many biological systems, movement of an organism occurs in response to a diffusible or otherwise transported signal, and in its simplest form this can be modeled by diffusion equations with advection terms of the form first derived by Patlak [*Bull. of Math. Biophys.*, 15 (1953), pp. 311–338]. However, other systems are more accurately modeled by random walkers that deposit a nondiffusible signal that modifies the local environment for succeeding passages. In these systems, one example of which is the myxobacteria, the question arises as to whether aggregation is possible under suitable hypotheses on the transition rules and the production of a control species that modulates the transition rates. Davis [*Probab. Theory Related Fields*, 84 (1990), pp. 203–229] has studied this question for a certain class of random walks, and here we extend this analysis to the continuum limit of such walks. We first derive several general classes of partial differential equations that depend on how the movement rules are affected by the local modulator concentration. We then show that a variety of dynamics is possible, which we classify as aggregation, blowup, or collapse, depending on whether the dynamics admit stable bounded peaks, whether solutions blow up in finite time, or whether a suitable spatial norm of the density function is asymptotically less than its initial value.

Key words. aggregation, blowup, collapse, chemotaxis equations, diffusion approximation, reinforced random walk

AMS subject classifications. 35Q80, 60J15, 65U05, 92B05 35B05, 35K50, 35K55

PII. S0036139995288976

1. Introduction.

1.1. Biological background. A characteristic feature of living systems is that they sense the environment in which they reside and respond to it. The response frequently involves movement toward or away from an external stimulus, and such a response is called a *taxis*, which stems from the Greek *taxis*, meaning *to arrange*. Taxis results when individuals change their pattern of movement, or *kinesis*, in response to the stimulus. It may be characterized as positive or negative, depending on whether it is toward or away from the external stimulus that affects the pattern of movement. Many different types of taxis are known, including aerotaxis, chemotaxis, geotaxis, haptotaxis, and others. The purposes of taxis range from movement toward food and avoidance of noxious substances to large-scale aggregation for the purpose of survival. The latter serves as a model for morphogenetic movements in general.

Any taxis involves two major components: (i) an external signal and (ii) the response of the organism to this signal. The response in turn involves two major steps: (i) detection of the signal and (ii) transduction of the external signal into an internal signal that controls the pattern of movement. At the individual level, one can distinguish between cases in which individuals change their direction of motion in response to the stimulus and cases in which they change the frequency of turning or

*Received by the editors July 12, 1995; accepted for publication (in revised form) March 13, 1996. http://www.siam.org/journals/siap/57-4/28897.html

†Department of Mathematics, University of Utah, Salt Lake City, UT 84112 (othmer@math.utah.edu). The research of this author was supported in part by NIH grant GM 29123.

‡Institut für Angewandte Mathematik, Universität Heidelberg, Im Neuenheimer Feld 294, 69120 Heidelberg, Germany (stevens@iwr.uni-heidelberg.de). The research of this author was supported in part by the Deutsche Forschungsgemeinschaft (SFB 123 and SFB 359).

the length of the "run" between reorientations. Both of these behavioral patterns can produce taxis at the population level. Another important aspect of taxis is whether or not the individual merely detects the signal or alters it as well, for example, by amplifying it so as to relay the signal. When there is no significant alteration, the individual simply responds to the spatiotemporal distribution of the signal. However, when the individual produces or degrades the signal, there is coupling between the local density of individuals and the intensity of the signal. This occurs, for example, when individuals aggregate in response to a signal from "organizers" and relay the signal as well.

In the majority of the theoretical analyses of taxis the signal is transported by diffusion, convection, or by some other means. However, there are instances in which the "walker" seems to modify the environment in a strictly local manner and there is little or no transport of the modifying substance. Examples include the myxobacteria, which produce slime over which their cohorts can move more readily, and ants, which follow trails left by predecessors. In either case, the question arises as to whether aggregation is possible with such strictly local modification or whether some form of longer range communication is necessary. Since we were first motivated to address this question by experiments on the myxobacteria, we shall describe their behavior in more detail and discuss some previous results on a stochastic automaton model for their motion that is based on a reinforced random walk.

1.2. An automaton model for the motion of myxobacteria. The myxobacteria are ubiquitous soil bacteria that glide on suitable surfaces or at air-water interfaces. Under starvation conditions they tend to glide close to one another. During gliding they form different patterns and finally aggregate to build so-called fruiting bodies. Inside these fruiting bodies they survive as dormant myxospores. The mechanisms by which myxobacteria glide on the substrate and aggregate are still not understood, and thus theoretical analysis of different mechanisms is useful. In this paper we focus on the trail-following behavior.

During gliding the myxobacteria produce so-called slime trails on which they prefer to glide. When a myxobacterium glides on bare substrate and encounters another slime trail at a relatively shallow angle, it will typically glide onto it. Once on the slime trail it increases its gliding velocity. In order to test the possible effects on aggregation of the slime-trail-following, a stochastic cellular automaton model was analyzed by Stevens [27], [28]. In this automaton, the bacteria are modeled as elongated objects with a realistic length-to-width relationship. They can glide on a square grid with periodic boundary conditions. In each time step new slime is produced under the entire cell body of each bacterium, and they all glide to one of their three nearest neighbors of their tip that is not occupied by their own cell body (doubling back is not allowed). If there is no slime on these spots for a bacterium, it will glide in the direction of its current orientation with a higher probability than in other directions. If there is slime on at least one of the neighboring spots, the probability to glide to one of them depends primarily on the slime density at these spots. The exact rules for this automaton are given in [27] and [28]. This model is a stochastic cellular automaton in the sense that there is a finite number of different states at each of the grid points and noise is added to the transition probabilities of the jump process. Although the jump process for a bacterium is not a Markov process, one gets a Markov process by including the slime as one of the state variables.

The results of the simulations with this stochastic cellular automaton show that the rules for slime-trail-following produce the observed preaggregation patterns but

do not lead to a final stable aggregation. Thus a number of bacteria aggregate simply by slime-trail-following, but these aggregates subsequently break up. Because of this effect, positive chemotaxis toward a diffusible substance was introduced into the model. Biological evidence for the existence of chemotaxis during myxobacterial aggregation is discussed by Dworkin and Kaiser [4]. In the model, after a fixed number of bacteria have aggregated by slime trail following, the bacteria begin to produce a diffusible chemical. The choice of directions is now supposed to depend on both the slime and the density of the diffusing chemical at the neighboring sites, and the effect of the chemoattractant is much stronger than the effect of the slime. With these additional rules, the automaton produces stable aggregation centers. In view of these results, we wanted to understand why slime-trail-following by itself does not account for aggregation in the cellular automaton and to determine if there are models in which it does.

Some insight in this problem can be gained from a result of Davis [3]. He considered a reinforced random walk for a single particle in one dimension. This random walk is closely related to the one used in the stochastic cellular automaton model for many bacteria in two dimensions. To describe his results, consider a nearest neighbor random motion $\vec{X} = X_0, X_1, ...$ on the integers. Initially there is a weight on each interval $(i, i+1),\ i \in \mathbb{Z}$, which is equal to 1. If at time n an interval has been crossed by the particle exactly k times, its weight will be $1+\sum_{j=1}^{k} a_j$, where $a_j \geq 0\ ,\ j = 1, ..., k$. If $(X_0, X_1, ..., X_n) = (i_0, i_1, ..., i_n)$ are given, then the probability that X_{n+1} is $i_n - 1$ or $i_n + 1$ is proportional to the weights at time n of the intervals $(i_n - 1, i_n)$ and $(i_n, i_n + 1)$.

Davis's main theorem asserts that localization of the particle will occur if the weight on the intervals grows quickly enough with each crossing. To be more precise, let $\vec{a} = a_1, a_2, ...$. Then if $\phi(\vec{a}) = \sum_{n=1}^{\infty} (1 + \sum_{j=1}^{n} a_j)^{-1} = \infty$ (e.g., $a_j =$ constant; *linear growth*), then $\vec{X}$ is recurrent almost surely, which means that all integers are visited infinitely often, almost surely.

If $\phi(\vec{a}) < \infty$ (e.g., $a_j = j$; *superlinear growth*), then $\vec{X}$ has finite range almost surely and there are (random) integers N and m such that $X_i \in \{m, m+1\}$ if $i > N$. Thus the particle oscillates between two random integers almost surely after some random elapsed time.

Since the result deals with a single particle, it does not directly address the aggregation issue, but it does at least suggest that if the particles interact only through the modification of the transition probability, there may be aggregation if this modification is strong enough.

The rules which were used in the stochastic cellular automaton model of bacterial trail-following are quite similar to the rules described above. One difference is that the slime is not deposited on the interval a bacterium has crossed but rather at the point where it is located. This makes a difference, as will be shown in the following simulations and in the continuum approximation of the jump process.

In order to make a direct comparison with Davis's result, a simplified stochastic cellular automaton is considered. Starting with a nearest neighbor random walk on the integers, one puts an initial weight equal to 1 on each integer (not on the intervals). If at time n an integer has been visited exactly k times, its weight will be $1+\sum_{j=1}^{k} a_j$, with $a_j \geq 0\ ,\ j = 1, ..., k$. In the following, Davis's reinforced random walk and this random walk are simulated for a single particle in two space dimensions. In contrast to the assumptions in [3], an upper bound for the slime on each integer is prescribed in both simulations.

FIG. 1. *Simulation of a random walk of one particle (black) in two dimensions on a periodic* 50×50 *grid, using Davis's movement rules and linear growth of the slime* ($a_j = 0.2, j = 1, 2, \dots$). *Gridpoints that have been visited at least once by a particle are marked by small gray squares. The figure shows the result after* 3000 *jumps, starting from the center point.*

The simulations of the two-dimensional jump process based on Davis's rules show that the particle ultimately oscillates between two points if the growth of the slime is exponential in the number of crossings. If the growth is linear with a small growth rate, the particle does not stay in a fixed finite region (cf. Figure 1). In these two cases, the results of the simulations agree qualitatively with the theoretical result, which is only proven for a one-dimensional system. If the growth is linear but the growth rate is too large, the results of the simulation are no longer comparable to the theoretical prediction, even in the one-dimensional case, because this approaches the borderline case between recurrence of the random walk and oscillation of the particle. The time for the particle to leave a fixed finite region grows as the growth rate of the slime increases.

If the two-dimensional simulations are done using the simplified stochastic cellular automaton rules instead of Davis's rules, one finds that the localization effect is stronger (cf. Figure 2).

Next these rules are used for many particles on a fixed two-dimensional grid with periodic boundary conditions. Initially, 1000 particles are randomly seeded on the 30×30 central square of the original grid. Each particle lays down slime in every time step, and the slime grows exponentially. Again the aim is to compare the results using Davis's rules with those from the simplified stochastic cellular automaton. The results are shown in Figures 3 and 4. Using Davis's rules one finds that after a short time each particle oscillates between two lattice sites, but only about three or four are concentrated at any pair of sites. If we use the same initial conditions in the simplified stochastic automaton, we find that particles also oscillate between two neighboring points of the grid after a short time, but now the local aggregates are larger. On average about 12 particles oscillate between the same two points, and of course fewer points are occupied by the particles (cf. Figures 3 and 4). Therefore there are rules for the simplified stochastic cellular automaton that do not involve long-range signaling and under which aggregation of many particles by slime-trail-following occurs. In

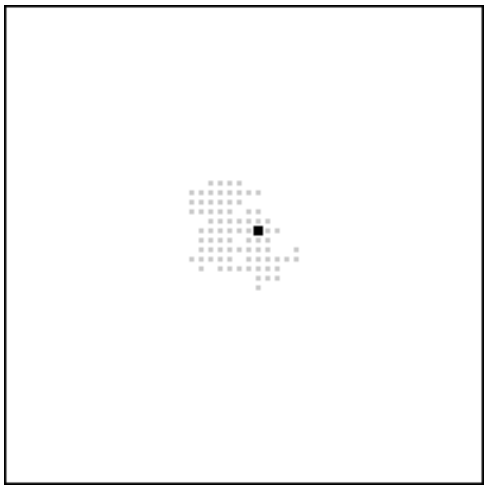

FIG. 2. *Simulation of a random walk of one particle in two dimensions on a periodic* 50×50 *grid, using the rules of the simplified cellular automaton model and linear growth of the slime* ($a_j = 0.2, j = 1, 2, \dots$). *The figure shows the sites visited after* 3000 *jumps. Clearly the particle visits fewer sites as compared with Figure* 1*, which implies that these rules tend to produce stronger localization.*

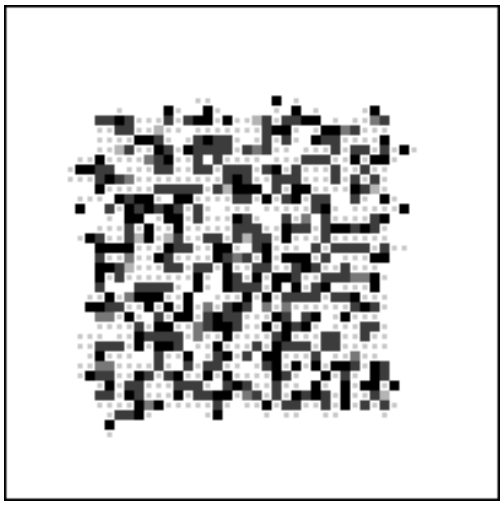

FIG. 3. *This figure shows the discrete density distribution for* 1000 *bacteria after* 1000 *jumps, using Davis's movement rules with* $a_1 = 1$ *and* $a_j = 1 + 1 + \sum_{k=1}^{j-1} a_k$. *The bacteria are interacting only via the slime trails. The density of bacteria is coded as follows: black for one bacterium at a grid point, dark gray for two to four bacteria, gray for five and six bacteria, and light gray for seven and more bacteria located at the same grid point. All grid points that have been visited by at least one bacterium are marked by smaller gray squares. All particles are quickly trapped in the sense that they soon oscillate between two points.*

the automaton the bacteria sense the slime on the nearest neighbors, whereas in Davis's case they sense the slime only at a distance of a half-step. This suggests that aggregation, as opposed to mere localization, requires longer-range sensing than what is suggested by Davis's one particle result.

However, when these rules of slime production are tested in the full stochastic cellular automaton, one finds that even this does not account for stable aggregation

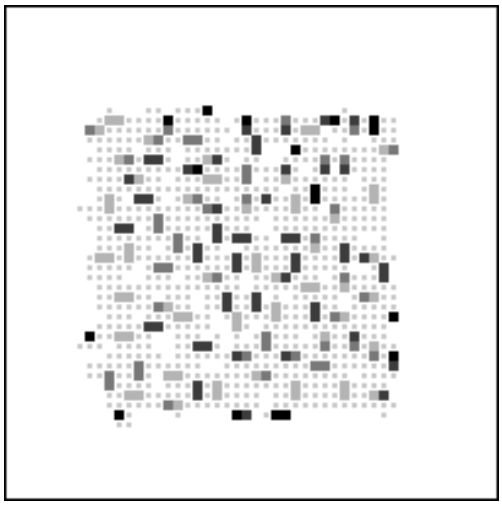

FIG. 4. *The density distribution using the rules for the simplified stochastic cellular automaton for* 1000 *bacteria after* 1000 *time-steps with* $a_1 = 1$ *and* $a_j = 1 + 1 + \sum_{k=1}^{j-1} a_k$. *The localization of the particles is stronger than in Figure* 3, *since more particles are trapped in most of the small areas than before.*

centers. The reasons for this must lie in additional factors suggested by the experiments, such as (i) the persistence in the movement of the bacteria or (ii) contacts between bacteria, which forces nearest neighbors to alter their gliding velocity.

1.3. Background on continuum descriptions of motion. In this paper we will analyze continuous approximations of the various jump processes with a view toward determining whether stable aggregation or blowup is possible without long-range signaling. To understand where our analysis fits into different approaches to modeling movement, let us first restrict attention to noninteracting particles. If the forces are deterministic and individuals are regarded as point masses, their motion can always be described by Newton's laws, and this leads to a classification of movement according to the properties of the forces involved. (Although the particles are regarded as structureless, we admit the possibility that they can exert forces.) First, if the forces are smooth bounded functions, the governing equations are smooth and the paths are smooth functions of time. In a phase space description in which the fundamental variables are position and velocity, Newton's equations are

$$\frac{d\mathbf{x}}{dt} = \mathbf{v}, \tag{1}$$

$$m\frac{d\mathbf{v}}{dt} = \mathbf{F}. \tag{2}$$

If we assume that the forces are independent of the velocity, then these are just the characteristic equations for the hyperbolic equation

$$\frac{\partial \rho}{\partial t} + \mathbf{v} \cdot \nabla_{\mathbf{x}} \rho + \frac{\mathbf{F}}{\mathrm{m}} \cdot \nabla_{\mathbf{v}} \rho = 0. \tag{3}$$

Here ρ is the density of individuals, defined so that $\rho(\mathbf{x}, \mathbf{v}, t) d\mathbf{x} d\mathbf{v}$ is the number of individuals with position and velocity in the phase volume $(d\mathbf{x} d\mathbf{v})$ centered at $(\mathbf{x}, \mathbf{v})$.

If we define the number density n and the average velocity $\mathbf{u}$ by

$$n(\mathbf{x},t) = \int \rho(\mathbf{x},\mathbf{v},t)d\mathbf{v}, \tag{4}$$

$$n(\mathbf{x},t)\mathbf{u}(\mathbf{x},t) = \int \rho(\mathbf{x},\mathbf{v},t)\mathbf{v}d\mathbf{v}, \tag{5}$$

then the evolution of these average quantities is governed by

$$\frac{\partial n}{\partial t} + \nabla_{\mathbf{x}} \cdot (n\mathbf{u}) = 0. \tag{6}$$

If we admit impulsive (i.e., distributional) forces, then we arrive at the second major type of movement, which is called a velocity jump process in [22]. In this case the motion consists of a sequence of "runs" separated by reorientations, during which a new velocity is chosen instantaneously. If we assume that the velocity changes are the result of a Poisson process of intensity λ, then in the absence of other forces we obtain the evolution equation

$$\frac{\partial \rho}{\partial t} + \nabla_{\mathbf{x}} \cdot \mathbf{v}\rho = -\lambda\rho + \lambda \int T(\mathbf{v},\mathbf{v}')\rho(\mathbf{x},\mathbf{v}',\mathrm{t})\, d\mathbf{v}'. \tag{7}$$

For most purposes one does not need the distribution ρ but only its first few velocity moments. If we integrate this over $\mathbf{v}$, we again obtain (6). Similarly, multiplying (7) by $\mathbf{v}$ and integrating over $\mathbf{v}$ give

$$\frac{\partial (n\mathbf{u})}{\partial t} + \nabla \cdot \int \rho\mathbf{v}\mathbf{v}\, d\mathbf{v} = -\lambda n\mathbf{u} + \lambda \int T(\mathbf{v},\mathbf{v}')\mathbf{v}\rho(\mathbf{x},\mathbf{v}',\mathrm{t})\, d\mathbf{v}'\, d\mathbf{v}. \tag{8}$$

This is an adequate description for the movement of many organisms, and examples of its application are given in [22].

The final description of motion, which in a sense is the roughest, is the familiar random walk, in which there are instantaneous changes in position at random times. These are called space-jump processes in [22], where it is shown that the probability density for such a process satisfies the integral equation

$$P(\mathbf{x},t|0) = \hat{\Phi}(t)\delta(\mathbf{x}) + \int_0^t \int_{R^n} \phi(t-\tau)T(\mathbf{x},\mathbf{y})P(\mathbf{y},\tau|0)\, d\mathbf{y}\, d\tau. \tag{9}$$

Here $P(\mathbf{x},t|0)$ is the conditional probability that a walker who begins at the origin at time zero is at $\mathbf{x}$ at time t, $\phi(t)$ is the density for the waiting time distribution, $\hat{\Phi}(t)$ is the complementary cumulative distribution function associated with $\phi(t)$, and $T(\mathbf{x},\mathbf{y})$ is the redistribution kernel for the jump process.

If the initial distribution is given by $F(\mathbf{x})$, then

$$n(\mathbf{x},t) \equiv \int_{R^n} P(\mathbf{x},t|\mathbf{x}_0)F(\mathbf{x}_0)\, d\mathbf{x}_0$$

can be regarded as the number density of identical noninteracting walkers at $\mathbf{x}$ at time t. Clearly $n(\mathbf{x},t)$ satisfies

$$n(\mathbf{x},t) = \hat{\Phi}(t)F(\mathbf{x}) + \int_0^t \int_{R^n} \phi(t-\tau)T(\mathbf{x},\mathbf{y})n(\mathbf{y},\tau)\, d\mathbf{y}\, d\tau. \tag{10}$$

If the support of the kernel $T(\mathbf{x}, \mathbf{y})$ is a lattice and the waiting time distribution is exponential, as in a Poisson process, then it is easy to see that (9) reduces to

$$\frac{\partial P}{\partial t}(x_i, t|0) = -\lambda P(x_i, t|0) + \lambda \sum_j T_{ij} P(\mathbf{x}_j, t|0). \tag{11}$$

Here λ is the parameter of the exponential distribution, and the sum is over the support of T. This is just a master equation for a continuous-time, discrete-space random walk. A generalization of it that incorporates state-dependent transition rates serves as the starting point for the derivations given in the following section.

An alternate approach in which the changes of position or velocity are not generated by a jump process postulates the presence of small fluctuating components of velocity and/or position. This leads to the familiar stochastic differential equations

$$\begin{aligned} d\mathbf{x} &= \mathbf{v}\mathrm{dt} + \mathrm{d}\mathcal{X}, \\ m d\mathbf{v} &= \mathbf{F}\mathrm{dt} + \mathrm{d}\mathcal{V}, \end{aligned} \tag{12}$$

where $\mathcal{X}$ and $\mathcal{V}$ are random displacements and velocities, respectively. This approach leads to a Fokker–Planck equation under suitable conditions on the fluctuating forces [12].

The situation is more complicated when particle interactions are taken into account (cf. [26], [20]). Thus, for instance, in the case of myxobacteria, a bacterium gliding on a slime trail reacts to its own contribution to this trail and to the contributions of the other bacteria. In [28] a rigorous derivation of density equations for the reaction of myxobacteria to a chemical which they produce is given. The reinforced random walk of one particle as used in the simplified cellular automaton is related to a Fokker–Planck equation that will be derived in the following sections. In [28] the stochastic equation, equivalent to this Fokker–Planck equation, was set up for the position of a bacterium and the chemical species was described by a diffusion process. Under certain regularity assumptions it was shown that the equation for the dynamics of the bacterial density corresponds to the probability density equation for the dynamics of a single bacterium if the self-interactions of the bacteria and their interaction with the chemical is moderate. This means that in the limit as the population size tends to infinity, the primary range of interaction for each bacterium must shrink to zero, but the number of other bacteria and chemical molecules within this range of interaction must tend to infinity.

To date, a similar derivation of density equations for a strictly local interaction of the particles instead of a moderate one has not been done. In [28] it was necessary to assume diffusion for the chemical, but the difficulty in repeating such a derivation of the density equations for myxobacteria reacting towards slime trails (which means a nondiffusing "chemical substance") is probably only a technical one. In this paper the particle motion is governed by a jump process, and our results can be rigorously interpreted only as equations for the probability density of a single particle or via the equivalent stochastic equation as a density equation when moderate interaction is taken into account.

With this in mind, we derive continuum descriptions that correspond to various rules for the motion of a particle on a one-dimensional lattice, beginning with a master equation for a continuous-time, discrete-space process. This leads to equations of the form

$$\frac{\partial p}{\partial t} = \frac{\partial}{\partial x}\left(D\frac{\partial p}{\partial x} - p\chi(w)\frac{\partial w}{\partial x}\right)$$

for the evolution of the probability density p. In addition there will be an evolution equation for the control or modulator substance w, but this does not diffuse. One of our objectives is to understand how the microscopic model for the response of an individual to the signal translates into the chemotactic sensitivity χ that appears in this equation. As we shall see, we are able to derive all the commonly used forms of the chemotactic sensitivity function from plausible assumptions about the microscopic models for the individuals' response. We analyze various combinations for the form of the taxis functional and the local dynamics, and we give examples of aggregation, blowup, and collapse.

In section 2 we derive the equations for the probability density, and in section 3 we discuss various forms of the local dynamics used in the simulations reported in section 4. For certain choices of the chemotactic response function and the local dynamics, the simulations suggest that the solutions blow up in finite time. In section 5 we analyze the effects of saturation in the response functional on the dynamics and show computationally that aggregation and collapse can exist for suitable choices of the functional.

2. The dynamics of movement. As we remarked in the introduction, we begin with a master equation for a continuous-time, discrete-space random walk. At the outset we consider only random walks on one-dimensional lattices, but the derivations extend to higher dimensions without change and we usually simply state the general result in each case. We postulate a generalized form of (11) in which the transition rates depend on the density of a control or modulator species that modulates the transition rates. We restrict attention to one-step jumps, although it is easy, using the framework given in the introduction, to generalize this (cf. [1]). However, one usually does not obtain diffusion equations in the continuum limit.

Suppose that the conditional probability $p_n(t)$ that a walker is at $n \in \mathbb{Z}$ at time t, conditioned on the fact that it begins at $n = 0$ at $t = 0$ and evolves according to the continuous-time master equation

$$\frac{\partial p_n}{\partial t} = \hat{\mathcal{T}}^+_{n-1}(W)\, p_{n-1} + \hat{\mathcal{T}}^-_{n+1}(W)\, p_{n+1} - (\hat{\mathcal{T}}^+_n(W) + \hat{\mathcal{T}}^-_n(W))\, p_n. \tag{13}$$

Here $\hat{\mathcal{T}}^\pm_n(\cdot)$ are the transition probabilities per unit time for a one-step jump to $n \pm 1$, and $(\hat{\mathcal{T}}^+_n(W) + \hat{\mathcal{T}}^-_n(W))^{-1}$ is the mean waiting time at the nth site. We assume throughout that these are nonnegative and suitably smooth functions of their arguments. The vector W is given by

$$W = (\dots, w_{-n-1/2}, w_{-n}, w_{-n+1/2}, \dots, w_o, w_{1/2}, \dots). \tag{14}$$

Note that the density of the control species w is defined on the embedded lattice of half the step size. The evolution of w will be considered in section 3; for now we simply assume that the distribution of w is given. Clearly a time- and p-independent spatial distribution of w can model spatial variation in the transition rates, but this case is not treated here.

As (13) is written, the transition probabilities can depend on the entire state and on the entire distribution of the control species. Since there is no explicit dependence on the previous state the process appears to be formally Markovian. However, if the evolution of w_n depends on p_n, as in section 3, then there is an implicit history dependence, and the space-jump process by itself is not Markovian. However, if one enlarges the state space by appending the slime concentration w, one gets a Markov process in this new state space.

To model movement in a finite domain we consider a finite segment $(-N, N)$ of the lattice and extend w and p as even functions about $-N$ and N. Under suitable conditions on $\hat{\mathcal{T}}$ this ensures that the net flux across the boundary is zero in the continuum limit of the one-dimensional problem, and as a result, the mass is conserved. For a general domain we later simply assume that the flux vanishes on the boundary.

There are three distinct types of models, which differ in the dependence of the transition rates on w, that we consider here: (i) strictly local models, (ii) barrier models, and (iii) gradient models. These are treated in the following subsections.

2.1. Transition rates based on local information. In the first scheme we assume that the mean waiting time at site n depends only on the density of the control species at that site. Since the transition probabilities are independent of the lattice site and depend only on the local densities, there is no source of spatial bias in the walk, so $\hat{\mathcal{T}}_n^{\pm}$ are equal and we denote them by $\hat{\mathcal{T}}(w_n)$. As a result (13) becomes

$$\frac{\partial p_n}{\partial t} = \hat{\mathcal{T}}(w_{n-1})\ p_{n-1} + \hat{\mathcal{T}}(w_{n+1})\ p_{n+1} - 2\hat{\mathcal{T}}(w_n)\ p_n. \tag{15}$$

We consider a grid of mesh size h, set $x = nh$, and expand the right-hand side as a function of x to second order in h and obtain

$$\frac{\partial p}{\partial t} = h^2 \frac{\partial^2}{\partial x^2}\left(\hat{\mathcal{T}}(w)\ p\right) + \mathcal{O}(h^4). \tag{16}$$

We assume that there is a scaling of the discrete transition rates such that $\hat{\mathcal{T}}(w) = \lambda \mathcal{T}(w)$ and such that the limit

$$\lim_{\substack{h\to 0\\ \lambda\to\infty}} \lambda h^2 = D$$

exists. Here λ has dimension t^{-1} and $\mathcal{T}(w)$ is now a dimensionless function. The diffusion limit of (15) is

$$\frac{\partial p}{\partial t} = D\frac{\partial^2}{\partial x^2}(\mathcal{T}(w)\ p), \tag{17}$$

and in higher space dimensions the analogue of (17) is

$$\frac{\partial p}{\partial t} = D\Delta(\mathcal{T}(w)\ p) \tag{18}$$

for $\mathbf{x} \in \Omega$, provided that the medium is homogeneous and isotropic. Here and hereafter we regard the diffusion limit as formal since we do not obtain the a priori bounds on higher derivatives needed to validate this limiting procedure. In particular, as we shall see later, there are solutions of the continuum equations for which this limit probably is not valid.

The evolution of p according to (18) is subject to initial and boundary conditions, and p should be nonnegative. If Ω is a bounded domain, then we suppose that the boundary is smooth and we suppose that the flux vanishes on the boundary. As a result, the solution of (18) must also satisfy the conservation condition

$$\int_\Omega p(\mathbf{x}, t)d\mathbf{x} = \int_\Omega p(\mathbf{x}, 0)d\mathbf{x} \equiv P_0 \tag{19}$$

for any bounded or unbounded one-, two-, or three-dimensional domain Ω. If Ω is infinite, we assume that the initial data has finite mass. Similar remarks apply to all the continuum equations derived in the remainder of this section.

The conservation law (18) can be written in the form

$$\frac{\partial p}{\partial t} + \nabla \cdot \mathbf{j} = 0, \tag{20}$$

where the particle flux for this process is

$$\mathbf{j} = -D\nabla(\mathcal{T}(w)\ p). \tag{21}$$

This can be written in the alternate form

$$\mathbf{j} = -D\mathcal{T}(w)\nabla p - Dp\mathcal{T}'(w)\nabla w, \tag{22}$$

and to conform with the conventional notation [25] we can write this as

$$\mathbf{j} = -D\mathcal{T}(w)\nabla p + p\chi(w)\nabla w, \tag{23}$$

where $\chi(w) \equiv -D\mathcal{T}'(w)$ is called the chemotactic sensitivity. If $\mathcal{T}'(w) \neq 0$, the flux contains both a diffusional component with coefficient $D\mathcal{T}(w)$ and a component due to taxis. When $\mathcal{T}'(w) < 0$, the tactic component of the flux is in the direction of ∇w and the taxis is positive. For the simple linear response given by $\mathcal{T}(w) = \alpha + \beta w$ with α and β nonnegative, the diffusion coefficient is $D(\alpha + \beta w)$ and the chemotactic sensitivity is simply $-D\beta$. Of course it may be more realistic to suppose that the response to w saturates at large w, and this can be described by $\mathcal{T}(w) = \alpha + \beta w/(\gamma + w)$, where $\gamma \geq 0$. In this case the chemotactic sensitivity is $\chi(w) = -D\beta\gamma/(\gamma + w)^2$. In either case the taxis is negative when $\beta > 0$, which reflects the fact that the mean waiting time at a site is a decreasing function of w, and thus particles tend to accumulate where w is small. If $\beta < 0$, the taxis is positive, but then the linear response is only meaningful for $w < \alpha/\beta$.

The average particle velocity, as defined by $\mathbf{j} = p\mathbf{u}$, is given by

$$\mathbf{u} = -D\mathcal{T}(w)\frac{\nabla p}{p} - D\mathcal{T}'(w)\nabla w. \tag{24}$$

This should be compared with the average velocity for a pure diffusion process ($\mathcal{T} \equiv 1$ in (21)), namely,

$$\mathbf{u} = -D\frac{\nabla p}{p}. \tag{25}$$

Consideration of the average particle velocity provides an alternate way to view positive and negative taxis: a taxis is positive when the component of the average velocity due to taxis (the taxis velocity for short) is in the direction of ∇w and negative otherwise.

When there is a nonzero taxis component in the motion, it can balance the diffusional component and lead to a nonconstant steady state of (18). At a steady state, $\mathcal{T}(w)p$ is harmonic, and if Ω is a bounded domain with homogeneous Neumann conditions on the boundary, then the steady-state solution of (18) is

$$p(\mathbf{x}) = \frac{P_0}{\mathcal{T}(w)(\mathbf{x})}\left(\int_\Omega \frac{d\Omega}{\mathcal{T}(w)(\mathbf{x})}\right)^{-1}. \tag{26}$$

In particular, if $w(\mathbf{x})$ is a specified nonconstant function, then the steady-state distribution of p is also nonconstant and the maxima of p coincide with the minima of $\mathcal{T}(w)$. If such a solution is stable, it represents an aggregation or a collapse, depending on the initial data of the time dependent problem. More precisely, we define aggregation, blowup, and collapse as follows.

DEFINITION 2.1. *Let $p(\mathbf{x},t)$ be the solution of an evolution equation such as* (18) *for a given initial distribution $p(\cdot,0)$. Then*

- *if* $\liminf_{t\to\infty}\|p(.,t)\|_{L_\infty} > \|p(.,0)\|_{L_\infty}$ *and* $\|p(.,t)\|_{L_\infty} <$ constant *for all t, we call this an* aggregation,
- *if* $\|p(.,t)\|_{L_\infty}$ *becomes unbounded in finite time, then we say that there is* blowup,
- *if* $\limsup_{t\to\infty}\|p(.,t)\|_{L_\infty} < \|p(.,0)\|_{L_\infty}$ *we say that there is* collapse.[1]

Clearly the definition does not preclude the possibility that all three cases may occur for the same equation, depending on the choice of initial data. Examples of these possibilities will be given later.

2.2. Barrier and nearest-neighbor models. In a barrier model we suppose that the w-dependence of the transition rate at site n is localized at $n\pm 1/2$. One may think of an interpenetrating set of barriers between the primary lattice sites whose ease of passage is governed by the density of w at that site. In these models the w-dependence gives rise to a bias in the transition rates at a point (i.e., the rates are not isotropic), and we should expect the resulting equation to contain terms that are not invariant under the transformation $x \to -x$. Two cases arise, depending on whether or not the transition rates are renormalized so that the mean waiting time at a site is constant.

When the transition rates depend only on the barrier to be crossed, a case which has been treated by others (see, e.g., [6], [21]), we write

$$\hat{\mathcal{T}}_n^{\pm}(W) = \hat{\mathcal{T}}(w_{n\pm 1/2}). \tag{27}$$

Using the same scaling as before we find that p evolves according to the equation

$$\frac{\partial p}{\partial t} = D\frac{\partial}{\partial x}\left(\mathcal{T}(w)\frac{\partial p}{\partial x}\right) \tag{28}$$

in one space dimension, where D is as previously given. The invariant form for any number of space dimensions is

$$\frac{\partial p}{\partial t} = D\nabla\cdot(\mathcal{T}(w)\nabla p). \tag{29}$$

The average particle velocity is

$$\mathbf{u} = -D\mathcal{T}(w)\frac{\nabla p}{p}, \tag{30}$$

and thus this process contains only a diffusional component; there is no directed motion and hence no taxis. In addition, if $\mathcal{T}(w) > 0$ it is easy to show that there are no nonconstant steady-state solutions; simply observe that $\mathcal{T}$ defines a new metric for Ω under which the steady-state version of (29) is Laplace's equation.

[1] The term collapse is sometimes used to denote what is called blowup here. Our terminology is consistent with that used for similar phenomena in other equations.

Lapidus [13] has studied the time evolution of solutions to equations of the form (29) for various initial data and has found that there may be transient "aggregation." However, this does not persist, as we would predict from the steady-state analysis. He calls this phenomenon "pseudochemotaxis." Both of the preceding cases are also discussed by Patlak [23], who gives references to earlier work.

The form of the transition rates given by (27) imposes no restriction on the transition rates at a site; they may take any value in $\mathbb{R}^+$, and there is no correlation between the transition rates to the right and left. However, we may also suppose that the decision when to jump is made independently of the decision where to jump, as in (9). If the mean waiting time at a site does not depend on w (or x), then it is constant across the lattice and the transition rates must be renormalized to reflect this. Thus

$$\hat{\mathcal{T}}_n^+(W) + \hat{\mathcal{T}}_n^-(W) = \text{constant}, \tag{31}$$

and without loss of generality we may suppose that the constant is equal to 2λ. To achieve this we can define[2]

$$\hat{\mathcal{T}}_n^{\pm}(W) = 2\lambda \frac{\mathcal{T}(w_{n\pm 1/2})}{\mathcal{T}(w_{n+1/2}) + \mathcal{T}(w_{n-1/2})} \equiv 2\lambda \mathcal{N}_n^{\pm}(W). \tag{32}$$

When $\mathcal{T}(w) = w$, this is the form used in the result due to Davis discussed earlier. Clearly this renormalization is uninteresting in the case in which the transition rates depend only on information at the site, for then (32) implies that $\mathcal{N}_n^{\pm}(w) = 1/2$. This is to be expected from the symmetry that exists in this case.

This renormalization introduces longer-range dependence of the transition rates on the control species, for now

$$\mathcal{N}_{n\pm 1}^{\mp}(w_{n\pm 1/2}, w_{n\pm 3/2}) = \frac{\mathcal{T}(w_{n\pm 1/2})}{\mathcal{T}(w_{n\pm 3/2}) + \mathcal{T}(w_{n\pm 1/2})}, \tag{33}$$

and the master equation (13) reads

$$\begin{aligned} \frac{1}{2\lambda}\frac{\partial p_n}{\partial t} &= \mathcal{N}^+(w_{n-1/2}, w_{n-3/2})\; p_{n-1} + \mathcal{N}^-(w_{n+1/2}, w_{n+3/2})\; p_{n+1} \\ &\quad - \left(\mathcal{N}^+(w_{n+1/2}, w_{n-1/2}) + \mathcal{N}^-(w_{n-1/2}, w_{n+1/2})\right) p_n. \end{aligned} \tag{34}$$

Here and hereafter we suppress the lattice index on $\mathcal{N}_n^{\pm}(\cdot,\cdot)$ because the underlying lattice is homogeneous. To obtain a diffusion equation from (34) we use the fact that $\mathcal{N}^+(u,v) = 1 - \mathcal{N}^-(v,u)$ and define $\mathcal{N} \equiv \mathcal{N}^+$. Then

$$\frac{\partial p}{\partial t} = D\frac{\partial}{\partial x}\left(\frac{\partial p}{\partial x} - 2p\left(\mathcal{N}_1 - \mathcal{N}_2\right)\frac{\partial w}{\partial x}\right), \tag{35}$$

where $D = \lim_{\substack{h\to 0 \\ \lambda\to\infty}} \lambda h^2$, $\mathcal{N}_k \equiv \partial_k \mathcal{N}(\cdot,\cdot)$, and ∂_k denotes a derivative with respect to the kth argument for $k = 1, 2$, evaluated at (w_n, w_n). It follows from (32) and (33) that

$$\mathcal{N}_1 = \frac{1}{4}\left(\ln \mathcal{T}(w)\right)'$$

[2]This is not just a rescaling in time but a new jump process.

and that $\mathcal{N}_2 = -\mathcal{N}_1$. Therefore (35) can be written in the alternate forms

$$\frac{\partial p}{\partial t} = D\frac{\partial}{\partial x}\left(\frac{\partial p}{\partial x} - p\frac{\partial}{\partial x}\ln\mathcal{T}(w)\right) \tag{36}$$

$$= D\frac{\partial}{\partial x}\left(p\frac{\partial}{\partial x}\left(\ln\frac{p}{\mathcal{T}(w)}\right)\right). \tag{37}$$

The chemotactic sensitivity is

$$\chi(w) = 2D\left(\mathcal{N}_1 - \mathcal{N}_2\right) = D\left(\ln\mathcal{T}(w)\right)', \tag{38}$$

and the average velocity is

$$\mathbf{u} = -D\frac{\partial}{\partial x}\ln p + D\left(\ln\mathcal{T}(w)\right)'\frac{\partial w}{\partial x}. \tag{39}$$

Thus the taxis is positive if $\mathcal{T}'(w) > 0$.

If we suppose that the transition rate is given by $\mathcal{T}(w) = \alpha + \beta w$, with $\beta > 0$, then one finds that

$$\mathcal{N}_1 = \frac{1}{4}\left(\frac{\beta}{\alpha + \beta w}\right)$$

and therefore

$$\frac{\partial p}{\partial t} = D\frac{\partial}{\partial x}\left(\frac{\partial p}{\partial x} - p\frac{\beta}{\alpha+\beta w}\frac{\partial w}{\partial x}\right) \tag{40}$$

$$= D\frac{\partial}{\partial x}\left(p\frac{\partial}{\partial x}\left(\ln\frac{p}{\alpha+\beta w}\right)\right). \tag{41}$$

We shall use this functional form of $\mathcal{T}(w)$ as a prototype for renormalized transition rates in section 4. Davis's result discussed earlier corresponds to the choice $\alpha = 0$, $\beta = 1$.

In two space dimensions we use a square grid, and analogous to (32), we define the renormalized transition probabilities as

$$\hat{\mathcal{T}}(u,v,y,z) = 4\lambda\frac{\mathcal{T}(u)}{\mathcal{T}(u)+\mathcal{T}(v)+\mathcal{T}(y)+\mathcal{T}(z)} \equiv 4\lambda\mathcal{N}(u,v,y,z).$$

The resulting master equation is the two-dimensional analog of (34). To simplify the notation we let $\mathcal{N}_k = \partial_k\mathcal{N}(\cdot,\cdot,\cdot,\cdot)$, $k = 1,2$, where the derivatives are evaluated at $(w_{n,m}, w_{n,m}, w_{n,m}, w_{n,m})$. Then we find that the diffusion limit of this master equation leads to the evolution equation

$$\frac{\partial p}{\partial t} = D\nabla\cdot\left(\nabla p - 4p\left(\mathcal{N}_1 - \mathcal{N}_2\right)\nabla w\right), \tag{42}$$

where $D = \lim_{\substack{h\to 0\\ \lambda\to\infty}} \lambda h^2$. One also finds that

$$4\left(\mathcal{N}_1 - \mathcal{N}_2\right) = \left(\ln\mathcal{T}(w)\right)',$$

and therefore (42) can be written

$$\frac{\partial p}{\partial t} = D\nabla\cdot\left(\nabla p - p\left(\ln\mathcal{T}(w)\right)'\nabla w\right) \tag{43}$$

$$= D\nabla\cdot\left(p\nabla\left(\ln\frac{p}{\mathcal{T}(w)}\right)\right), \tag{44}$$

which has the same form as the corresponding equation (37) for one space dimension.

Clearly the renormalization of a barrier model has a very significant effect: it introduces a taxis when compared to a barrier model without renormalization, and the chemotactic sensitivity is quite different from that for strictly local sensing. Here $\chi(w) = D(\ln\mathcal{T}(w))'$ and the taxis is positive if $\mathcal{T}'(w) > 0$.

For the original and the simplified stochastic cellular automaton one deals with a renormalized nearest-neighbor model. A generalized description of the random walk simulated in Figure 1 yields the following transition rates:

$$N_n^{\pm}(W) = \frac{\mathcal{T}(w_{n\pm1})}{\mathcal{T}(w_{n+1}) + \mathcal{T}(w_{n-1})}\,. \tag{45}$$

The diffusion limit in this case is

$$\frac{\partial p}{\partial t} = D\frac{\partial}{\partial x}\left(\frac{\partial p}{\partial x} - 2p(\ln\mathcal{T}(w))'\frac{\partial w}{\partial x}\right), \tag{46}$$

and therefore the chemotactic sensitivity is $2D(\ln\mathcal{T}(w))'$. In the original and simplified stochastic cellular automaton we used $\mathcal{T}(w) = w$, so the chemotactic sensitivity is $2D/w$, which is twice that in Davis's case. This may explain the differences between the localization behavior of one particle and the aggregation of many particles shown in Figures 1 and 2 and Figures 3 and 4, respectively. This result suggests that the bacteria must have a certain perception range to be able to aggregate, but a single particle will localize for a smaller perception range.

2.3. Gradient-based (nonlocal) models. If the "organism" probes the local environment before making a decision as to how to move, then the transition rates may depend on the difference between w at the current point and the nearest neighbor in the direction of movement. For simplicity we treat only linear dependence on nearest-neighbor differences, but the results can easily be generalized. Suppose that in one space dimension

$$\begin{aligned}\hat{\mathcal{T}}_{n-1}^{+}(W) &= \alpha + \beta(\tau(w_n) - \tau(w_{n-1})),\\ \hat{\mathcal{T}}_{n+1}^{-}(W) &= \alpha + \beta(\tau(w_n) - \tau(w_{n+1})),\end{aligned} \tag{47}$$

where $\alpha \geq 0$. One easily shows that for this choice of the transition rates the invariant form of the evolution equation is

$$\frac{\partial p}{\partial t} = D\left(\alpha\Delta p - 2\beta\nabla\cdot(p\tau'(w)\nabla w)\right). \tag{48}$$

Equation (48) can also be written in the form

$$\frac{\partial p}{\partial t} = D\nabla\cdot\left[p\left(\frac{\alpha\nabla p}{p} - 2\beta\tau'(w)\nabla w\right)\right], \tag{49}$$

and thus the average particle velocity is

$$\mathbf{u} = D\left[-\frac{\alpha\nabla p}{p} + 2\beta\tau'(w)\nabla w\right] \tag{50}$$

and the chemotactic sensitivity is

$$\chi(w) = 2D\beta\tau'(w). \tag{51}$$

TABLE 1
Dependence of the response on the sensing mechanism.

	Type of sensing	Taxis velocity	Chemotactic sensitivity	Type of taxis
1.	Local	$-D\nabla\mathcal{T}$	$-D\mathcal{T}'(w)$	Negative if $\mathcal{T}'(w) > 0$
2.	Barrier without renormalization	0	0	None
3.	Barrier with renormalization	$D\nabla ln\mathcal{T}$	$D\left(\ln\mathcal{T}(w)\right)'$	Positive if $\mathcal{T}'(w) > 0$
4.	Nearest neighbor with renormalization	$2D\nabla ln\mathcal{T}$	$2D\left(\ln\mathcal{T}(w)\right)'$	Positive if $\mathcal{T}'(w) > 0$
5.	Gradient without renormalization	$2D\beta\nabla\tau$	$2D\beta\tau'(w)$	Positive if $\beta\tau'(w) > 0$
6.	Gradient with renormalization	$D\frac{\beta}{\alpha}\nabla\tau$	$D\frac{\beta}{\alpha}\tau'(w)$	Positive if $\beta\tau'(w) > 0$

Thus the taxis is positive or negative according to whether $\beta\tau'(w)$ is positive or negative. The diffusion component of the velocity vanishes if there is no basal transition rate ($\alpha = 0$).

If $\alpha > 0$, the transition rates can be renormalized so that their sum is one pointwise and (48) is replaced by

$$\frac{\partial p}{\partial t} = D\nabla \cdot \left\{ \frac{1}{2}\nabla p - p\frac{\beta\tau'(w)}{\alpha}\nabla w \right\}. \tag{52}$$

Other types of nonlocal schemes are possible. For instance, one may suppose that the difference in $\tau(w)$ only provides the direction, and hence (47) should be divided by the modulus of the difference. In another possible scheme the transition rate could be determined only by w at the destination. We leave the derivation of the governing equations for these cases to the reader.

For comparison purposes, we summarize the results of this section in Table 1.

To illustrate the differences between the mechanisms more concretely, let us suppose that the control species binds to a receptor R and that the complex transduces the external signal into an internal signal. Further, suppose that the response is proportional to the fraction of receptors occupied. The binding reaction may be written

$$R + w \underset{k_{-1}}{\overset{k_1}{\rightleftarrows}} [Rw], \tag{53}$$

where $[Rw]$ denotes the receptor-signal complex. If binding equilibrates rapidly on the time scale of the evolution of p and w, then for the local sensing model and the barrier model we may suppose that

$$\mathcal{T}(w) = \beta\frac{w}{\gamma + w}, \tag{54}$$

where β is a constant that incorporates the total number of receptors and $\gamma \equiv k_{-1}/k_1$. For a gradient model we may set $\tau(w)$ equal to the ratio on the right-hand side of (54). One then has

$$\nabla\tau(w) = \frac{\beta\gamma}{(\gamma + w)^2}\nabla w, \tag{55}$$

whereas for a barrier and a nearest-neighbor model with renormalization one has

$$\nabla \ln \mathcal{T}(w) = \frac{\gamma}{w(\gamma + w)} \nabla w. \tag{56}$$

Thus the taxis velocities and sensitivities will have very different behaviors when $w << \gamma$, depending on the type of model used.

3. The local dynamics for the control species. Davis's results and the two-dimensional simulations in Figures 1 and 2 suggest that the asymptotic behavior of the probability density p for one particle, or analogously the density equation interpreted as a limiting equation for moderately interacting bacteria, may depend strongly on the dynamics of w. In particular the growth of w determines whether or not blowup occurs. In the following section we consider several different combinations of chemotactic sensitivities and production rates for w. In this section we summarize the three types of dynamics considered for w. We scale the time and, where necessary, w so as to make the leading coefficient equal to one.

(I) Linear growth:

$$\frac{dw}{dt} = p - \mu w. \tag{57}$$

Here we suppose that production of w is proportional to the local density of p. Davis's result for $\mu = 0$ and equation (40) would suggest that this growth is too slow to lead to blowup.

(II) Exponential growth:

$$\frac{dw}{dt} = (p - \mu) w. \tag{58}$$

Here the control species grows exponentially, and Davis's result for $\mu = 0$ and equation (40) would suggest that blowup may occur.

(III) Saturating growth:

$$\frac{dw}{dt} = \frac{pw}{(1 + \nu w)} - \mu w + \gamma_r \frac{p}{1 + p}. \tag{59}$$

Saturation in the production of the control species is certainly more realistic in the biological context. In the above form the production can locally be very large if ν is sufficiently small, but eventually it saturates. In addition, there is a w-independent production. As we shall see, these factors produce very interesting behavior in the p equation.

4. Analytical and numerical results on stability and asymptotic dynamics. In this section we obtain some analytical results on the local behavior of solutions of the partial differential equations which result from the diffusion approximation of the jump processes discussed earlier. We also numerically simulate these equations. The main objectives are to determine whether or not aggregation, blowup, or collapse occurs, how the asymptotic dynamics depend on the chemotactic sensitivity, the production rate of the control species and the initial data, and how the results compare with the simulations done for the associated jump processes with one or many particles. From the standpoint of the application which motivated this study, we want to determine the conditions under which myxobacteria may be able

to aggregate solely as a result of following slime trails, i.e., in the absence of any long-range communication via a diffusible substance.

Throughout this section we consider a barrier model with linear response function and renormalized transition rates, and we first consider one space dimension. The governing equation for the particle density is equation (40):

$$\frac{\partial p}{\partial t} = D\frac{\partial}{\partial x}\left(\frac{\partial p}{\partial x} - p\frac{\beta}{\alpha+\beta w}\frac{\partial w}{\partial x}\right) \qquad \text{for} \qquad x \in (0,1) \tag{60}$$

with boundary conditions

$$p\frac{\partial}{\partial x} ln\left(\frac{p}{\alpha+\beta w}\right) = 0 \qquad \text{for} \qquad x = 0,1 \tag{61}$$

and initial data $p(x,0) = p_0(x)$. Until otherwise stated, $\beta > 0$, and when it is we may set it equal to 1. The time scale and the constants on the right are rescaled as necessary to reflect the scaling of the equations for the local dynamics.

In the following subsections we analyze the behavior of solutions of this equation for the three types of local dynamics given in section 3. In each case one can establish the existence of smooth solution for smooth initial data locally in time, and one can show that $(p(x,t), w(x,t)) \geq (0,0)$ if $(p_0(x), w_0(x)) \geq (0,0)$ by a maximum principle argument. We will not do this here but instead will focus on the asymptotic behavior of solutions.

4.1. Type I local dynamics. If the local dynamics for w are given by (57) and $\mu > 0$, then the system comprising (60), (61), and (57) has the constant solution $(p,w) = (p_0, p_0/\mu)$ for any $p_0 > 0$. If $\mu = 0$, then there is no time-independent solution, but there is a space-independent solution $(p,w) = (p_0, w_0 + p_0 t)$, provided that $p(x,0) \equiv p_0$ and $w(x,0) \equiv w_0$. A translation of Davis's result for linear growth to the continuum context is that both constant solutions should be stable. However, in the following proposition we prove that the former solution is asymptotically stable and the latter is unstable.

PROPOSITION 4.1. *If $\mu > 0$ and $\alpha > 0$, the constant solution $(p,w) = (p_0, p_0/\mu)$ of* (60), (61), *and* (57) *is asymptotically stable. If $\mu = 0$, the space-independent solution $(p_0, w_0 + p_0 t)$ is unstable for any $\alpha \geq 0$.*

Proof. First suppose that $\mu > 0$ and $\alpha > 0$, and let

$$\begin{aligned} p(x,t) &= p_0 + \xi(x,t), \\ w(x,t) &= w_0 + \eta(x,t), \end{aligned} \tag{62}$$

where $w_0 \equiv p_0/\mu$. Set $\Lambda = \beta p_0/(\alpha + \beta w_0)$; then the linearized evolution equations are

$$\frac{\partial \xi}{\partial t} = D\frac{\partial}{\partial x}\left(\frac{\partial \xi}{\partial x} - \Lambda\frac{\partial \eta}{\partial x}\right), \tag{63}$$

$$\frac{d\eta}{dt} = \xi - \mu\eta, \tag{64}$$

with boundary conditions

$$\frac{\partial \xi}{\partial x} - \Lambda\frac{\partial \eta}{\partial x} = 0. \tag{65}$$

A Fourier analysis of solutions of this system shows that all solutions tend to zero as $t \to \infty$ if and only if

$$\mu\alpha > 0.$$

If $\mu = 0$, then linearization around the space-independent solution leads to the system

$$\frac{\partial \xi}{\partial t} = D\frac{\partial}{\partial x}\left(\frac{\partial \xi}{\partial x} - \Lambda(t)\frac{\partial \eta}{\partial x}\right), \tag{66}$$

$$\frac{d\eta}{dt} = \xi, \tag{67}$$

where Λ is now time-dependent. We may solve the second equation and use the solution to rewrite the first equation as

$$\frac{\partial \xi}{\partial t} = D\frac{\partial^2 \xi}{\partial x^2} - D\Lambda(t)\int_0^t \frac{\partial^2 \xi}{\partial x^2}(x,s)ds. \tag{68}$$

Here we have assumed, without loss of generality that $\eta_{xx}(x,0) = 0$. We assume a solution of (68) of the form

$$\xi(x,t) = \phi(t)\cos(kx)$$

and find that ϕ is a solution of the equation

$$\phi'(t) = -k^2 D\phi + k^2 D\Lambda(t)\int_0^t \phi(s)ds.$$

This may be written as the system

$$\Phi' = \begin{bmatrix} -k^2 D & k^2 D\Lambda(t) \\ 1 & 0 \end{bmatrix}\Phi\ , \tag{69}$$

where $\Phi_1 \equiv \phi$ and $\Phi_2 \equiv \int_0^t \phi(s)ds$. The asymptotic behavior of the solution can be determined by appeal to the following theorem due to Hartman and Wintner [7] (cf. [5]).

THEOREM 4.2. *Consider the linear system*

$$x' = (\Delta(t) + R(t))\,x, \tag{70}$$

where Δ is a diagonal matrix. Suppose that the eigenvalues of Δ are such that for $i, j \in \{1, \dots, n\}$, whenever $i \neq j$

$$|Re\{\lambda_i(t) - \lambda_j(t)\}| \geq \delta$$

for some $\delta > 0$ and $t \in [a, \infty)$. Further suppose that the entries of R satisfy

$$\int_a^\infty |R_{ij}|^p dt < \infty \tag{71}$$

for some $p \in (1, 2]$. Then (70) has solutions $x_{(m)}(t)$ with the asymptotic form

$$x_{(m)}(t) = \{e_m + o(1)\}e^{\int_a^t \{\lambda_m(t) + R_{mm}(t)\}dt} \tag{72}$$

for $t \to \infty$, where e_m is the mth vector in the canonical basis for $\mathbb{R}^n$.

To apply this result, we define $x_1 = \frac{\Omega\phi_1}{k^2 D}$ and $x_2 = \phi_2 + \frac{\phi_1}{k^2 D}$. Then (69) can be written as

$$\frac{dx}{dt} = \begin{bmatrix} -k^2 D & 0 \\ 0 & 0 \end{bmatrix} x + \Lambda(t) \begin{bmatrix} -1 & \Omega \\ -\frac{1}{\Omega} & 1 \end{bmatrix} x, \tag{73}$$

where $\Omega \equiv \sqrt{1 + (k^2 D)^2}$. Clearly the second matrix satisfies (71) for any $p > 1$, since $\Lambda(t) \equiv \beta p_0/(\alpha + \beta w_0 + \beta p_0 t)$. Thus there is one exponentially decaying solution, but the solution corresponding to the zero eigenvalue requires closer examination. That solution has the form

$$x_{(2)} = \{e_2 + o(1)\} e^{\int_a^t \Lambda(s) ds}\ , \tag{74}$$

and the exponential factor is

$$\frac{\alpha + \beta w_0 + \beta p_0 t}{\alpha + \beta w_0 + \beta p_0 a}\ . \tag{75}$$

It follows that the solution of (70) corresponding to the zero eigenvalue is given by

$$\Phi_{(2)} = \{e_2 + o(1)\} \left(\frac{\alpha + \beta w_0 + \beta p_0 t}{\alpha + \beta w_0 + \beta p_0 a} \right) \tag{76}$$

as $t \to \infty$. Therefore $\Phi_{(2),2} \equiv \int_0^t \phi(s) ds \sim \mathcal{O}(t)$ as $t \to \infty$, so $\phi \sim \mathcal{O}(1)$, and the result follows. □

This result shows that growth of the control species proportional to the local density of the particles is not rapid enough to cause instability of the constant uniform solution when $\mu > 0$. Computational experiments show that for a wide variety of initial data, type I dynamics lead to collapse, and we conjecture that they always do when $\mu > 0$. The asymptotic behavior of solutions in the case $\mu = 0$ is also unknown, but our computations suggest the existence of small-amplitude stable solutions. An example using $D = 3.6 \times 10^{-2}$ and $\alpha = 0$ is shown in Figure 5. Here and hereafter, solutions are computed by discretizing the spatial derivatives using centered differences and solving the resulting system of ordinary differential equations using the stiff integrator package LSODE. To conserve particles, it is important to discretize the divergence form of the partial differential equation rather than expand the derivatives and discretize the resulting equation. Unless stated otherwise, all computational results are for a uniform grid of 201 points. We do not show w in this figure, but it is clear from (57) that asymptotically w grows linearly in t at the pointwise rate $p(x)$.

4.2. Type II local dynamics. The results are quite different for type II dynamics. First, the space-independent solution is catastrophically unstable in the sense that the unstable manifold is infinite dimensional. To simplify the analysis we set $\alpha = 0$ and first consider the case $\mu = 0$. Later we remark on the effect of $\alpha \neq 0$ and $\mu \neq 0$.

PROPOSITION 4.3. *The space-independent solution*

$$(p_0, w_0 e^{p_0 t}) \tag{77}$$

of the system

$$\begin{aligned} &\frac{\partial p}{\partial t} = D \frac{\partial}{\partial x} \left(\frac{\partial p}{\partial x} - \frac{p}{w} \frac{\partial w}{\partial x} \right), \\ &\frac{dw}{dt} = pw \end{aligned} \qquad \text{for} \quad x \in (0,1) \tag{78}$$

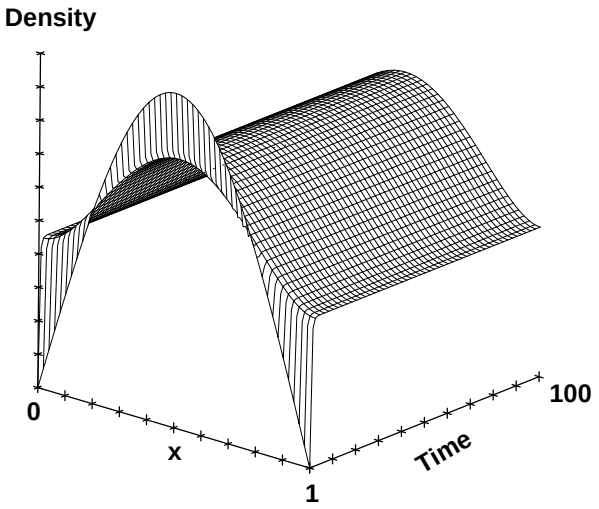

FIG. 5. *The dynamics of the system* (57), (60), *and* (61) *with* $\mu = \alpha = 0$, $D = 0.036$, *and* 201 *grid points. The initial Gaussian distribution for the bacterial density is* $p(x,0) = 4e^{-2(x-0.5)^2}/(2\pi)^{0.5}$. *The initial maximum is* 1.596, *and the asymptotic maximum is* 1.465. *In the context of myxobacteria, this behavior can be compared to what is called "swarming," where bacteria that are initially concentrated spread out as time evolves.*

with boundary conditions

$$p\frac{\partial}{\partial x} ln\left(\frac{p}{w}\right) = 0 \qquad for \qquad x = 0, 1 \tag{79}$$

and initial data $p(x,0) \equiv p_0 > 0$, $w(x,0) \equiv w_0 > 0$ *is unstable.*

Proof. The linearized equation governing small perturbations of the basic solution is

$$\frac{\partial \xi}{\partial t} = D\frac{\partial}{\partial x}\left(\frac{\partial \xi}{\partial x} - \Lambda(t)\frac{\partial \eta}{\partial x}\right), \tag{80}$$

$$\frac{d\eta}{dt} = p_0\eta + w_0 e^{p_0 t}\xi \ , \tag{81}$$

where $\Lambda(t) \equiv p_0 e^{-p_0 t}/w_0$. The solution of the second equation is

$$\eta(t) = e^{p_0 t}\eta(x,0) + e^{p_0 t}w_0 \int_0^t \xi(x,s)ds,$$

and therefore, if we assume that $\eta_{xx}(x,0) \equiv 0$, (80) becomes

$$\frac{\partial \xi}{\partial t} = D\frac{\partial}{\partial x}\left(\frac{\partial \xi}{\partial x} - p_0 \int_0^t \frac{\partial \xi}{\partial x}\right). \tag{82}$$

We may assume a solution of the form $\xi(x,t) = \phi(t)\cos(kx)$ and then find that ϕ satisfies

$$\phi^{'} = -k^2 D\phi + p_0 k^2 D \int_0^t \phi(s)ds. \tag{83}$$

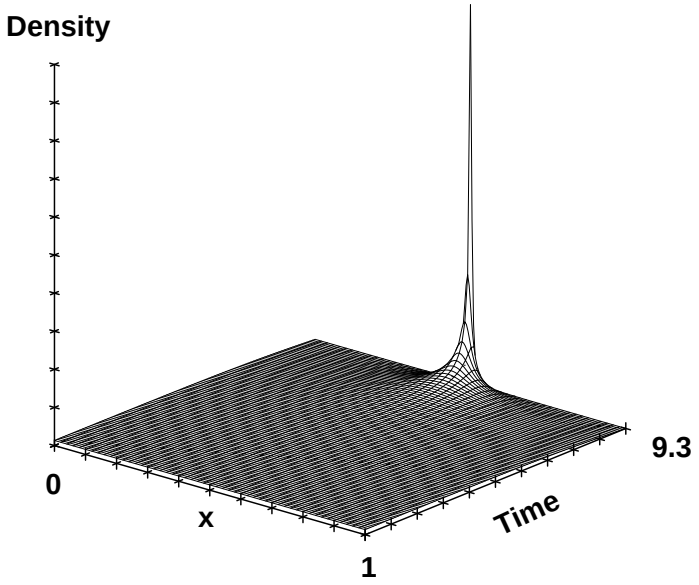

FIG. 6. *The dynamics of the system* (78), (79), *and* (58), *using* $\mu = \alpha = 0, D = 0.036$, *and a grid of* 201 *points. The initial data are* $p(x,0) = 1 - 0.01\cos(2\pi x), w(x,0) \equiv 1$. *Initially the peak decreases, which cannot be seen in the figure, but then recovers and apparently blows up in finite time.*

It follows that

$$\phi(t) = c_+ e^{\lambda^+ t} + c_- e^{\lambda^- t},$$

where $\lambda^\pm$ are given by

$$\lambda^\pm = \frac{-k^2 D \pm \sqrt{k^4 D^2 + 4p_0 k^2 D}}{2}.$$

The result follows from this, since $\lambda^+ > 0$ for all $k \neq 0$, and $k = 0$ is not admissible in light of the conservation condition. □

Since all wave numbers are unstable, the unstable manifold of any spatially uniform solution is infinite dimensional. Furthermore, since λ^+ is monotone increasing in k^2, the shortest wavelengths grow most rapidly. Since $p(x,t) \geq 0$ for $t \geq 0$ as long as the solution exists, w must always become unbounded in the sense that given any $W > 0$, there exists a time $T > 0$ such that

$$\sup_{x \in (0,1)} w(x,t) > W \tag{84}$$

for $t > T$. Numerical solution of the equations suggests that in fact blowup occurs in finite time for $\mu = 0$. The results of one simulation are shown in Figure 6.

The results shown are for 201 grid points and initial data comprising the second cosine mode, with an amplitude of 1% of the mean of p. The total mass becomes concentrated in a sharp spike centered at the maximum in the initial data. To check whether this is a numerical artifact, we monitor the total mass, which is conserved to within a few percentage points in all the results reported here. For instance, for the solution shown in Figure 6 the total mass at $t = 0$ is 200.9900, whereas at $t = 9.3$ it

is 200.3284. We have also done a similar computation using 401 and 801 grid points, with the same result: the entire mass becomes concentrated at a few points at the center of the interval. Initial data with two or three equally spaced maxima produce two or three points of concentration. Similar tests with initial data comprising the first 10 cosine modes, with random amplitudes chosen from $[0, 0.01]$, also produce numerical blowup. In all cases the total mass is conserved to within a few percentage points. Thus we believe that the underlying partial differential equation has solutions that blow up when the control species grows according to (58) with $\mu = 0$.

To test how strong the growth must be to produce blowup, we have also done simulations using the production $pw^{0.1}$. If we reduce D to 3.6×10^{-4} and use initial data with a single maximum, for instance, the initial peak in p first decreases but then recovers and finally blows up in finite time. It appears that blowup results whenever there is weak, nonsaturating, superlinear growth and no decay of the control species. These results are similar to Davis's result in that superlinear growth produces localization of the particle in the jump process and blowup in the continuum description.

To gain some insight into these results we shall consider the amplitude equations for a Fourier decomposition of the solution. For this purpose we assume that $w_0(x, 0) \equiv$ constant as in the simulation shown in Figure 6. Then we may write (78) as

$$\frac{\partial p}{\partial t} = D\left[\frac{\partial^2 p}{\partial x^2} - \frac{\partial p}{\partial x}\int_0^t \frac{\partial p}{\partial x} ds - p\int_0^t \frac{\partial^2 p}{\partial x^2} ds\right], \tag{85}$$

and, in view of the Neumann boundary conditions, we can assume a solution of the form

$$p(x,t) = \sum_{n=0}^{\infty} a_n(t)\cos(n\pi x). \tag{86}$$

If we define $b_n(t) \equiv \int_0^t a_n(s)ds$ for $n \geq 1$, then the amplitude equations can be written

$$\begin{aligned}\frac{da_n}{dt} = D\Big(&-(n\pi)^2 a_n + \frac{n\pi^2}{2}\sum_{k=0}^{n-1}(n-k)a_k b_{n-k} \\ &+ \frac{n\pi^2}{2}\sum_{k=0}^{\infty}\left[(n+k)a_k b_{n+k} - k a_{n+k} b_k\right]\Big),\end{aligned} \tag{87}$$

for $n = 1, 2, \ldots$. These equations show again that there are no steady states other than $a_0 \equiv$ constant, $a_k \equiv 0, k = 1, 2, \ldots$. This system decomposes into the following subsystems for the even and odd modes:

$$\begin{aligned}\frac{da_{2q}}{dt} = D\Bigg(&-(2q\pi)^2 a_{2q} + q\pi^2 \sum_{k=0}^{2q-1}(2q-k)a_k b_{2q-k} \\ &+ q\pi^2 \sum_{k=0}^{\infty}\left[(2q+k)a_k b_{2q+k} - k a_{2q+k} b_k\right]\Bigg),\end{aligned} \tag{88}$$

$$\begin{aligned}\frac{da_{2q+1}}{dt} = D\Bigg(&-((2q+1)\pi)^2 a_{2q+1} + (2q+1)\frac{\pi^2}{2}\sum_{k=0}^{2q}(2q+1-k)a_k b_{2q+1-k} \\ &+ (2q+1)\frac{\pi^2}{2}\sum_{k=0}^{\infty}\left[(2q+1+k)a_k b_{2q+1+k} - k a_{2q+1+k} b_k\right]\Bigg)\end{aligned}$$

for $q = 0, 1, 2, \ldots$. Since one odd index occurs in each product on the right-hand side of the second equation, it is clear that if $a_{2q+1}(0) = 0$ for all $q = 0, 1, 2, \ldots$, then $a_{2q+1}(t) \equiv 0$. Thus "energy" does not flow from the even to the odd modes if the amplitudes of the latter are all initially zero. Since the simulations show that apparent blowup occurs even if the initial data contain only even modes, we assume hereafter that the amplitudes of the odd modes are identically zero. Since $a_0 =$ constant, we may rewrite (88) and the equation for b_{2q} in the following form:

$$\frac{d}{dt}\begin{pmatrix} a_{2q} \\ b_{2q} \end{pmatrix} = \begin{bmatrix} -D(2q\pi)^2 & D(2q\pi)^2 a_0 \\ 1 & 0 \end{bmatrix} \begin{pmatrix} a_{2q} \\ b_{2q} \end{pmatrix} + 2Dq\pi^2 Q_{2q} \tag{89}$$

for $q \geq 1$, where

$$Q_{2q} = \begin{pmatrix} \displaystyle\sum_{k=1}^{q-1} (q-k) a_{2k} b_{2(q-k)} + \sum_{k=1}^{\infty} \left[(q+k) a_{2k} b_{2(q+k)} - k a_{2(q+k)} b_{2k} \right] \\ 0 \end{pmatrix}.$$

The linear part of this equation gives further insight into the mechanism of instability of the constant solution. The origin is a saddle point for the linear system associated with (89) and the unstable (stable) manifold for each q lies in the first/third (second/fourth) quadrants. Furthermore the instability is fed by the basic solution through a_0: if $a_0 = 0$, the trivial solution has an infinite-dimensional center manifold, and it is easy to see that all solutions of the linear system are bounded for all time. If we start with initial data comprising only the second mode ($q = 1$), then the instability in higher modes can only be triggered when the corresponding $a_{2q} \neq 0$ (and hence $b_{2q} \neq 0$). Some insight into the mechanism for energy flow between modes can be gained by examining the first few equations in this system. The a component of the first three equations, truncated so as to close the system, is as follows:

$$\frac{da_2}{dt} = D\left(-(2\pi)^2 a_2 + (2\pi)^2 a_0 b_2 + 2\pi^2 \left[2a_2 b_4 - a_4 b_2 + 3a_4 b_6 - 2a_6 b_4\right]\right), \tag{90}$$

$$\frac{da_4}{dt} = D\left(-(4\pi)^2 a_4 + (4\pi)^2 a_0 b_4 + 4\pi^2 \left[a_2 b_2 + 3a_2 b_6 - a_6 b_2\right]\right), \tag{91}$$

$$\frac{da_6}{dt} = D\left(-(6\pi)^2 a_6 + (6\pi)^2 a_0 b_6 + 6\pi^2 \left[2a_2 b_4 + a_4 b_2\right]\right). \tag{92}$$

Suppose that $a_2(0) \neq 0$ and $a_4(0) = a_6(0) = 0$. Then the fourth mode is excited via the term $a_2 b_2$, which in turn triggers the instability in the fourth mode via the linear mechanism. As soon as $a_4 \neq 0$ (which of course is instantaneously), mode six can be excited via the term $2a_2 b_4 + a_4 b_2$, and this in turn triggers the linear instability in the sixth mode. In this way there is a cascade in which the linear instability in successive modes is triggered by energy flow from lower modes. Obviously there is a complicated "back-and-forth" in that the flow is not unidirectional: a nonzero a_4 and a_6 affect a_2 through the term $2a_2 b_4 - a_4 b_2 + 3a_4 b_6 - 2a_6 b_4$, and this complicated interplay has prevented us from proving any global results about the dynamics of the amplitude equations to date. However, we have done a Fourier analysis of the numerical solution of the partial differential equation which qualitatively confirms the foregoing picture (cf. Figure 7). This figure shows the temporal evolution of $\log(a_k^2(t))$ for $k = 0, 2, \ldots, 8$. Initially only $a_2(0) \neq 0$, but the other modes grow rapidly and appear to converge to 1 at the blowup time. We have done a similar computation for the first 20 even modes with similar results: all amplitudes appear to converge to 1 at

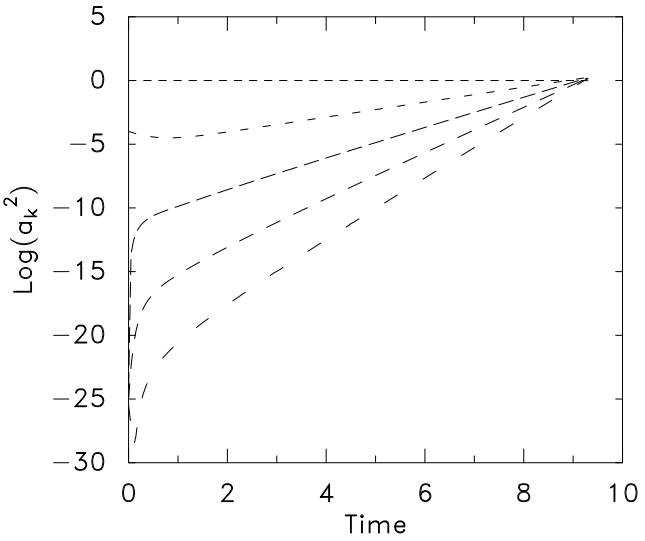

FIG. 7. *The evolution of the first five even Fourier amplitudes $a_0, \ldots, a_8$ for the solution shown in Figure* 6. *The amplitudes are shown in order of their index from top to bottom for t small, and this order is preserved in the evolution.*

the blowup time. This of course suggests that the solution approaches a δ-distribution at the blowup time.[3]

The results thus far pertain to the renormalized transition rate with $\alpha = 0$, and the question arises as to whether blowup occurs for a nonzero α. We have done computations with several positive values of α and have found that blowup occurs in all cases when the local dynamics are of type II, but the blowup time does depend weakly on α. Thus the presence or absence of the basal transition rate does not affect the general conclusion that blowup occurs when w grows according to (58).

Another question concerns the effect of the decay rate μ on whether or not blowup occurs, and if it does, on the time to blowup. Table 2 shows that there is no effect: within numerical accuracy the "blowup time" (determined by failure of the integrator to continue with a fixed error tolerance) and the maximum density at that time are independent of μ.

Of course, when $\mu > 0$ there is also a constant solution $(p_0, w_0) = (\mu, w_0)$ for any $w_0 > 0$, but later we show that such solutions are unstable as a consequence of Proposition 5.1.

The effect of the initial data on blowup is also of interest, since in some systems it is known that sufficiently large initial data are needed to produce blowup. However, in Proposition 4.3 we showed that a space-independent solution is linearly unstable to all wave numbers, and this suggests that there may be no threshold effect for the blowup. We have computed the solution of (78) for a variety of initial data, containing either a single mode of varying amplitude or random components. The "blowup" time depends strongly on the initial data, but in all cases the solution appears to blow up. Thus it appears that the only attractor for the forward evolution has essentially the

[3]Levine and Sleeman [14] have shown that for a special choice of initial data that is close to what we use in the computations one can construct an exact solution of (78) and (79). They prove that this solution blows up at a finite time T, with $p(\frac{1}{2}, t) \sim (T - t)^{-1}$ and that $p(x, t)$ approaches a δ function at the blowup time.

TABLE 2
Dependence of the blowup time on the decay rate μ for Type II *local dynamics with $\alpha = 0$.*

μ	Numerical blowup time	$p_{\max}$	$p_{\min}$
0.0	9.45	1.540079D+02	3.049632D-07
0.01	9.44	1.531900D+02	1.438778D-06
0.1	9.43	1.523350D+02	5.935083D-06
1.0	9.45	1.534283D+02	7.550620D-07

entire mass concentrated at a point when the initial data contain a single peak or at a finite set of points when the initial data have several local maxima. The dependence of the final distribution of mass on the initial distribution in the latter case has not been investigated thoroughly.

Stevens [29] has also done some preliminary computations in two space dimensions, and the results are similar to those in one space dimension. For instance, simulations in which the initial peaks are located sufficiently far apart from each other show that both can blow up in finite time. If two peaks are sufficiently close together initially, the larger one will engulf the smaller one. If both peaks have identical profiles initially, they either both blow up or form a new single peak. These results are similar to what is seen in one space dimension (results not shown), but there may be other phenomena in two space dimensions that are not seen in one space dimension. The two-dimensional results indicate that the model predicts behavior that is very similar to what is observed experimentally in the aggregation of myxobacteria, where the developing mounds may wax and wane before stabilizing in an aggregation.

4.3. Type III local dynamics. In the previous section we dealt with blowup of solutions. In this section we present some results on how changes in the net production rate of the modulator species w affect the asymptotic dynamics. This is a first step toward understanding how the rules for movement and for the production of the modulator may interact to produce aggregation, which is the primary case of interest in the biological context. In Figure 8 we show the solution of

$$\frac{\partial p}{\partial t} = D\frac{\partial}{\partial x}\left(\frac{\partial p}{\partial x} - \frac{p}{w}\frac{\partial w}{\partial x}\right) \quad \text{for} \quad x \in (0,1), \tag{93}$$

$$\frac{dw}{dt} = \frac{pw}{1+\nu w} - \mu w + \gamma_r \frac{p}{1+p} \quad \text{for} \quad x \in (0,1), \tag{94}$$

with Neumann boundary conditions for $\nu = 1 \times 10^{-5}$, $\mu = 0$, and $\gamma_r = 0$. To get a clearer picture of the evolution of p and w, we show the spatial profiles at a sequence of times in Figure 9.

The computational results shown in these figures suggest that p has reached a stable, stationary, nonconstant solution, whereas w continues to grow. Further evidence for this is shown in Figure 10, where in (a) we show the value of p at the midpoint of the interval as a function of time and in (b) we show the amplitudes of the first five even Fourier modes as a function of time. The results in Figure 8 suggest that

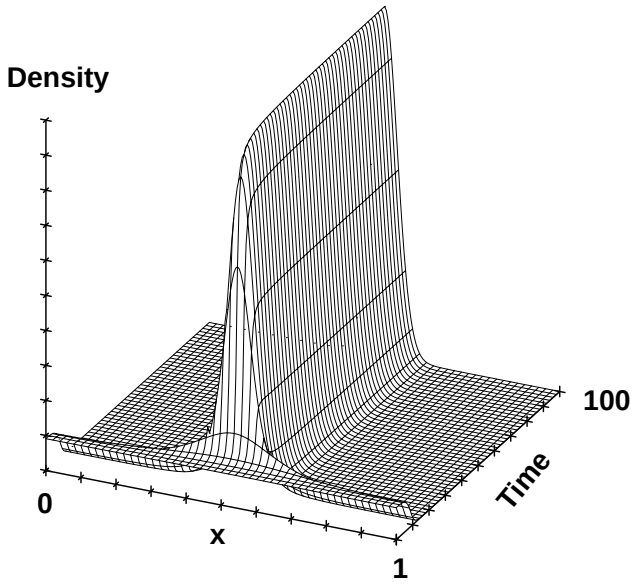

FIG. 8. *The evolution of p in* (93), (94) *as a function of time for* $D = 0.036$, $\nu = 1. \times 10^{-5}$, *and* $\mu = \gamma_r = 0$. *The initial data are as in Figure* 6.

we should look for solutions of the form

$$\begin{aligned} p(x,t) &= P_0(x), \\ w(x,t) &= A(t)P_0(x), \end{aligned} \tag{95}$$

where P_0 and A are unknown functions. Clearly solutions of this form satisfy (93) and (94) for any P_0, provided that A satisfies

$$A' = \frac{AP_0}{1 + \nu A P_0} - \mu A \, . \tag{96}$$

This equation can be solved for A in terms of P_0, but of course P_0 is determined by the initial data and can be determined only by solving the full evolution problem. Nonetheless, this shows how one can understand the results given in Figures 8 and 10. In particular, when $\mu = 0$, (96) shows that the w component of the solution at the midpoint of the interval in Figure 9(a) grows linearly in t for sufficiently large t, and the results in the figure can be checked against this. This behavior is similar to that shown in Figure 5, for when p stabilizes the growth rate of w is linear in t.

The decay rate μ of the control species has a very significant effect when the production rate saturates, as is shown in Figure 11. There we show the density p at the midpoint of the interval as a function of time for three different values of μ. When the decay rate is zero ($\mu = 0$), the density converges to a stable aggregation, and at intermediate values ($\mu = 0.1$) it grows slowly, but when $\mu = 1$ the solution appears to blow up in finite time.

The blowup at sufficiently large μ can be qualitatively understood from the fact that a large decay rate sharpens the w profile, which strengthens the chemotactic transport, which in turn leads to a sharpening of the p and hence w distributions. Moreover, at large μ the production of w never saturates, as can be seen by setting

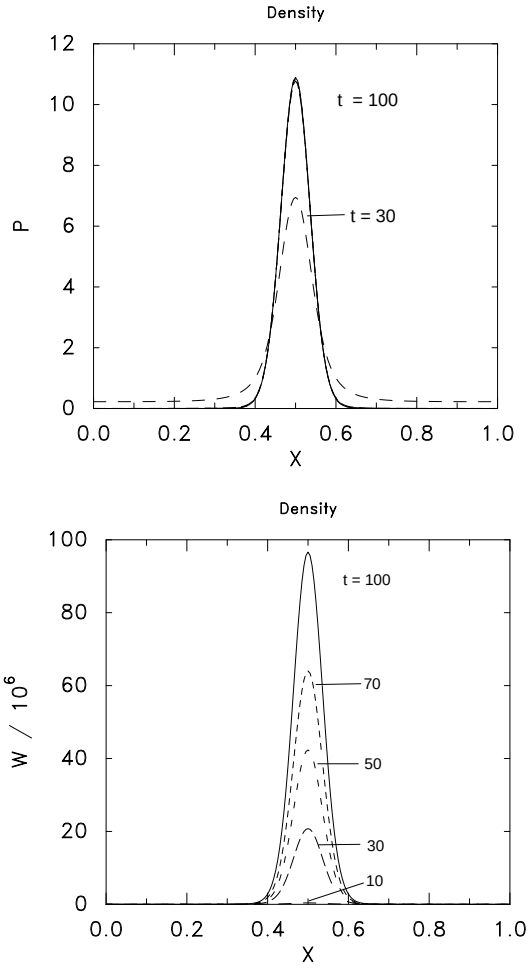

FIG. 9. *The spatial profiles of* p (a) *and* w (b) *at a sequence of times for the solution shown in Figure* 8.

$z = e^{\mu t} w$ in (94). Under these conditions the behavior is similar to that for type II dynamics.

Thus type III local dynamics can produce either stable aggregation or blowup, depending on the decay rate of the control species, and saturation of the production rate of the control species is essential for the former. In the following section we examine the effect of saturation in the response to the control species.

5. Saturation in the response functional. The receptor model that leads to (54) incorporates saturation in the response, but we shall first generalize this to include a basal transition rate. We write

$$\mathcal{T}(w) = \alpha + \beta_0 \frac{w}{\gamma + w} \tag{97}$$

$$\equiv (\alpha + \beta_0) \frac{\beta + w}{\gamma + w} \ , \tag{98}$$

where $\beta \equiv \alpha\gamma/(\alpha + \beta_0)$. In this section we consider only a barrier model with a renormalized transition rate, in which case the chemotactic sensitivity is given by

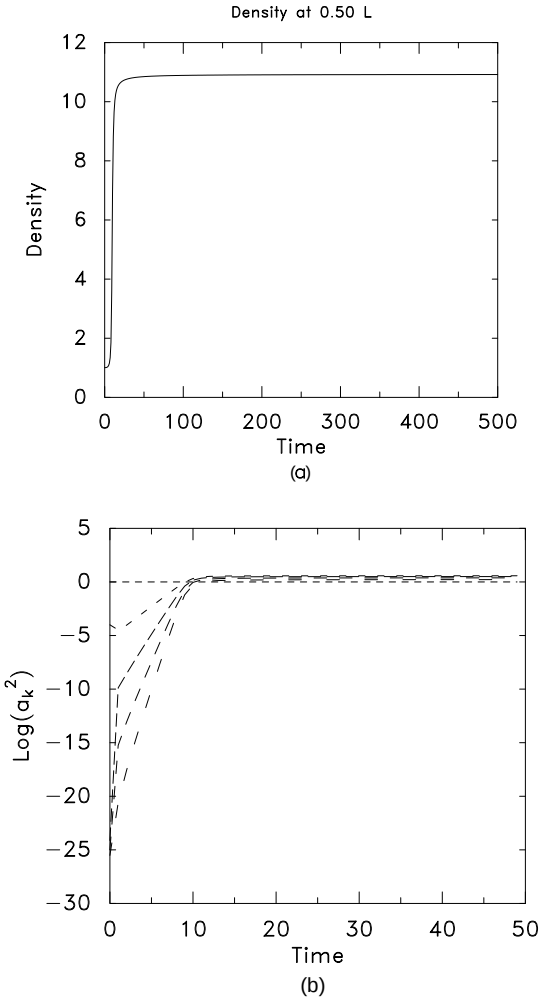

FIG. 10. (a) *The evolution of p for the solution shown in Figure* 8 *at the midpoint of the interval as a function of time.* (b) *The corresponding evolution of the amplitudes of the first five even Fourier modes, ordered by index from top to bottom for t small.*

$$\begin{aligned}\chi &= D(\ln \mathcal{T})_w \\ &= D\frac{\gamma-\beta}{(\gamma+w)(\beta+w)} \\ &\equiv D\frac{\delta}{(\gamma+w)(\beta+w)}\ .\end{aligned} \tag{99}$$

It is clear from the definition of β that $\delta > 0$, and thus the taxis is positive. We consider type II and III local dynamics, and thus the governing equations are

$$\begin{aligned}&\frac{\partial p}{\partial t} = D\frac{\partial}{\partial x}\left(\frac{\partial p}{\partial x} - p\frac{\delta}{(\gamma+w)(\beta+w)}\frac{\partial w}{\partial x}\right) \quad \text{for} \quad x \in (0,1), \\ &\frac{dw}{dt} = \frac{pw}{1+\nu w} - \mu w + \gamma_r \frac{p}{1+p} \quad \text{for} \quad x \in (0,1),\end{aligned} \tag{100}$$

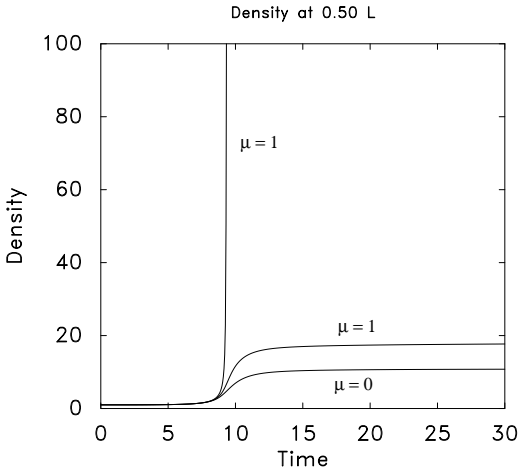

FIG. 11. *The evolution of p for the solution of* (93) *and* (94) *at the midpoint of the interval as a function of time for the indicated values of the decay rate* μ.

with Neumann boundary conditions. Throughout this section we set $\delta = \gamma = 1 \times 10^3$ and $\beta = 1 \times 10^{-2}$ unless otherwise stated. That we set $\delta = \gamma$ rather then have them differ by β is of no consequence.

We first set $\nu = 0$, in which case there is no saturation in the production rate of w. In Proposition 4.3 we showed that for $\mu = 0$ the uniform solution $(p_0, w_0 e^{p_0 t})$ of (78) is unstable, and numerical results suggest that solutions blow up in finite time. In Figure 12 we show the solution of (100) for $\nu = \mu = \gamma_r = 0$ and other parameters as above. The solution grows initially but then collapses and converges to the spatially uniform solution in which $p(x) \equiv 1$ and w grows exponentially. This suggests that a solution in which p, and hence w, is uniform may be stable when saturation in the response is incorporated, but we only prove this in case w is also a constant.

PROPOSITION 5.1. *Suppose that* $\nu > 0$ *and* $\gamma_r = 0$ *and that the system* (100) *has a constant solution* $(p, w) = (p_0, w_0)$, *where* $p_0 = \mu(1 + \nu w_0)$. *Then that solution is asymptotically stable if* $\mu > 0$ *and* p_0/μ *is sufficiently large.*

Proof. The linearized equation governing small perturbations of the basic solution is

$$\frac{\partial \xi}{\partial t} = D \frac{\partial}{\partial x} \left(\frac{\partial \xi}{\partial x} - \Lambda \frac{\partial \eta}{\partial x} \right), \tag{101}$$

$$\frac{d\eta}{dt} = \frac{w_0}{1 + \nu w_0} \xi + \left(\frac{p_0}{(1 + \nu w_0)^2} - \mu \right) \eta \ , \tag{102}$$

where $\Lambda \equiv \delta\mu(1 + \nu w_0)/(\gamma + w_0)(\beta + w_0)$. We may assume a solution of the form $(\xi(x,t), \eta(x,t)) = \phi e^{\lambda t} \cos(kx)$, where $\phi \in \mathbb{R}^2$; then λ is an eigenvalue of the matrix

$$L = \begin{bmatrix} -k^2 D & k^2 D \Lambda \\ \dfrac{w_0}{1 + \nu w_0} & \dfrac{\mu}{(1 + \nu w_0)} - \mu \end{bmatrix} . \tag{103}$$

It is easy to see that $\det L > 0 \Longrightarrow \text{trace} L < 0$ and that the former is equivalent to

$$\Upsilon > 1 + \frac{\delta \nu^2 \Upsilon(\Upsilon - 1)}{(\Upsilon + \gamma\nu - 1)(\Upsilon + \beta\nu - 1)} \ , \tag{104}$$

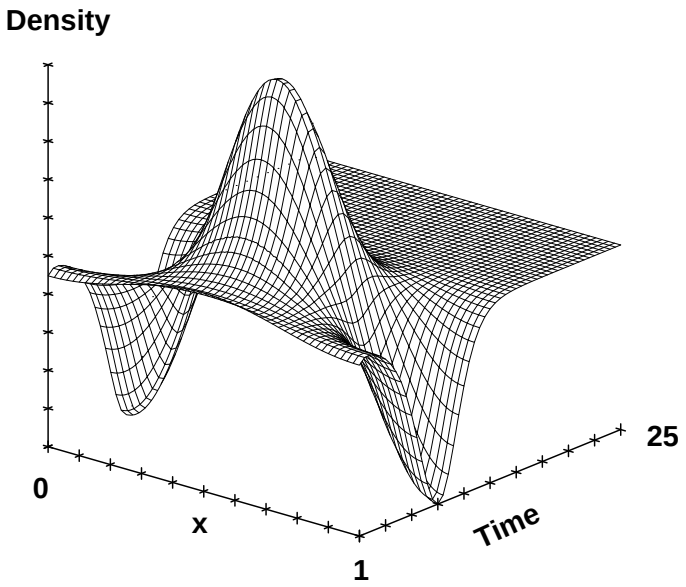

FIG. 12. *The evolution of p for the solution of* (100) *for* $D = 0.036$, $\nu = \gamma_r = \mu = 0$. *The initial data are as in Figure* 6. $p_{peak} = 1.139$.

where $\Upsilon \equiv p_0/\mu$. This can always be satisfied for sufficiently large Υ, which proves the result. □

Remark. When $\nu = 0$, $p_0 = \mu$, and $w_0 > 0$ is arbitrary, it follows that $\det L < 0$, which proves the assertion made earlier for type II dynamics.

There are also nonconstant solutions when $\mu > 0$. If we set $\mu = 1.0$, $\nu = \gamma_r = 0$, and compute the solution of (100) using the same parameters and initial data as in Figure 12, we obtain the result shown in Figure 13. Initially the saturation in the response is not significant and the solution "almost" blows up, but the saturation prevents this and the solution converges to the essentially piecewise-constant solution shown in that figure. Changing the initial perturbation on p from $-0.01\cos(2\pi x)$ to $-0.1\cos(2\pi x)$ does not alter the asymptotic value of p, but it does affect the maximum value of w in the interval at any fixed value of t. Earlier we saw that solutions of (78) appear to blow up for this value of μ (cf. Table 2). Thus saturation in the taxis response can produce stable aggregation as compared with blowup in its absence. Incorporation of saturation in the production of w by setting $\nu = 1 \times 10^{-5}$ produces an identical solution to within four decimal places, both in p_{peak} and in $p_{max}(\infty)$. Obviously piecewise-constant solutions satisfy (100), and one can prove that they are stable to perturbations that respect the discontinuities. Whether they are stable to general perturbations is not known.

However, saturation in the response does not preclude extreme concentration of the mass, as the solution shown in Figure 14 demonstrates. In this figure the initial value of w is reduced to 1.0×10^{-3} and the decay rate is set at $\mu = 1.0$. For this initial condition the solution remains essentially uniform in space for the first 62 time units but then begins to grow explosively in the center as in Figure 6. However, the growth is checked by the saturation in the response and the solution grows steadily and smoothly until essentially all the mass is concentrated at one point. If we repeat the computation using twice as many grid points (401), we again find that the mass

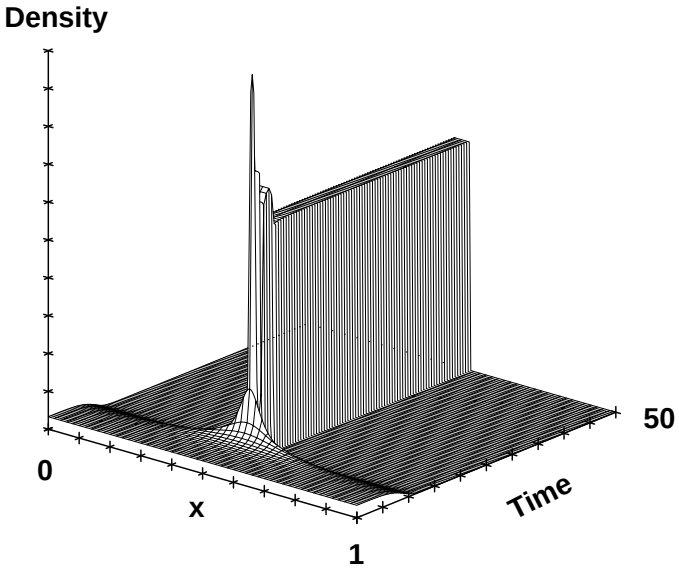

FIG. 13. *The evolution of p for the solution of* (100) *with* $\gamma_r = \nu = 0$ *and* $\mu = 1$. *The initial data are as in Figure* 6. $p_{peak} = 30.15$, $p_{min}(50) = 1.82 \times 10^{-4}$, $p_{max}(50) = 18.18$.

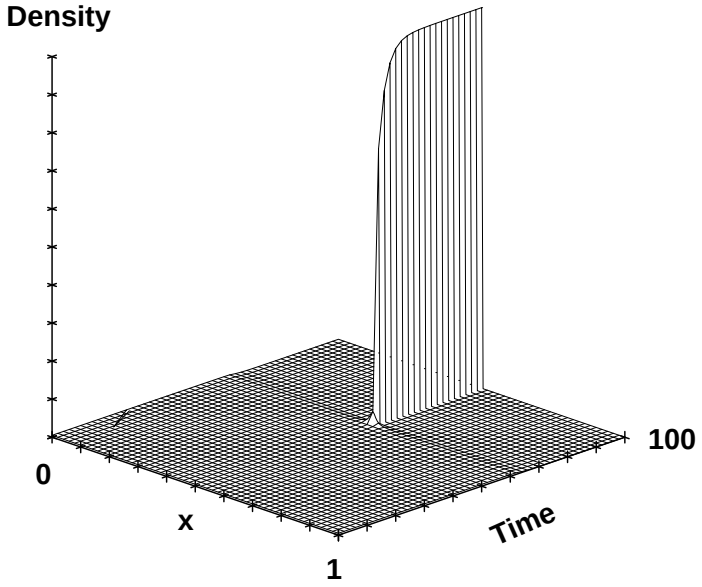

FIG. 14. *The evolution of p for the solution of* (100) *with* $\nu = 1 \times 10^{-5}$ *and* $\mu = 1$. *The initial data are as in Figure* 6 *for p, but w is set to* $1. \times 10^{-3}$ *everywhere.* $p_{min}(100) = 1.97 \times 10^{-3}$, $p_{max}(100) = 199.6$.

is all concentrated at one grid point. In both cases the mass is conserved to the same accuracy as in Figure 6. Thus we consider this a blowup, but from a computational standpoint it occurs much more smoothly than for the solution shown in Figure 6.

One might expect a blowup of the type shown in Figure 6 to occur if β is zero in (100), for then the chemotactic sensitivity would behave like $1/w$ for small w.

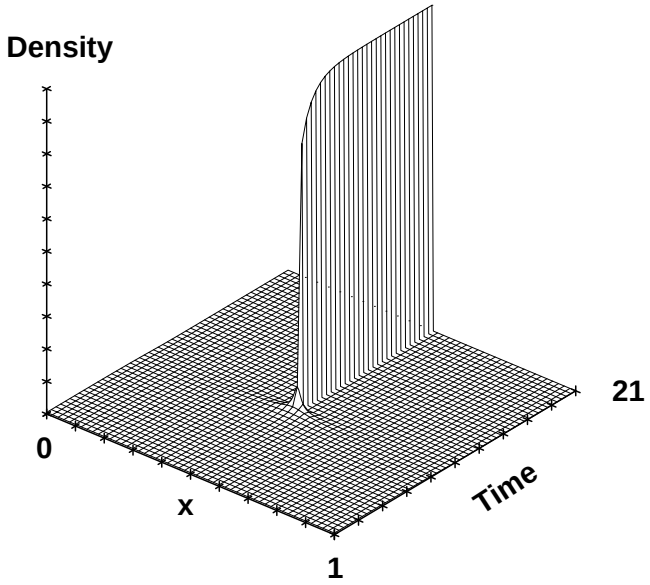

FIG. 15. *The evolution of p for the solution of* (100) *with* $\nu = 1 \times 10^{-5}$, $\beta = 0$, *and* $\mu = 1$. *Initial data are as in Figure* 14. $p_{min}(21) = 3.0 \times 10^{-7}$, $p_{max}(21) = 199.99$.

However, this is not sufficient, as can be seen in Figure 15. The solution grows more rapidly as compared with that shown in Figure 14, but the asymptotic profile is identical: essentially all the mass is concentrated at a single point. Thus the large w behavior is also important in determining whether or not the solution blows up, and a chemotactic sensitivity that behaves like w^{-2} for large w is strong enough to stabilize the solution sufficiently to allow it to be continued computationally. Similar results are obtained if the initial density of w is reduced. For instance, if we set all parameters to the values used in Figure 15 but reduce $w(x, 0)$ to 1×10^{-4}, we obtain a solution that "almost" blows up at $t = 9.35$, just as in Figure 6, but then stabilizes as in Figure 15 (results not shown). However, if we set the decay rate μ to zero, then the solution collapses, as is shown in Figure 16.

Thus there is a strong interplay between the chemotactic sensitivity, the production rate of the control species, and the initial data for w. A large decay rate or a small initial value of w promotes aggregation or blowup, whereas in the absence of decay the solutions tend to collapse. As a result, one would predict that a higher initial average density of p would tend to stabilize solutions that would blow up for smaller initial p or produce collapse for those solutions that would tend to a stable aggregation at a lower density, because more w is produced pointwise. An example that illustrates this is shown in Figure 17. The stable aggregate shown there should be compared with the blowup shown in Figure 15. The only difference between these is that the mean density of p in the former is twice that in the latter. It should also be compared with Figure 14. If we reduce the initial value of both p and w, we expect rapid aggregation or blowup, but if we also set μ equal to zero, we would predict that the solution collapses. These competing tendencies are illustrated in the solution shown in Figure 18. This solution initially grows but then settles into a sequence of decreasing plateaus in the maximum amplitude that eventually leads to collapse. Finally, if we repeat the computations for Figure 17 but set $\gamma_r = 0.1$, then there is a

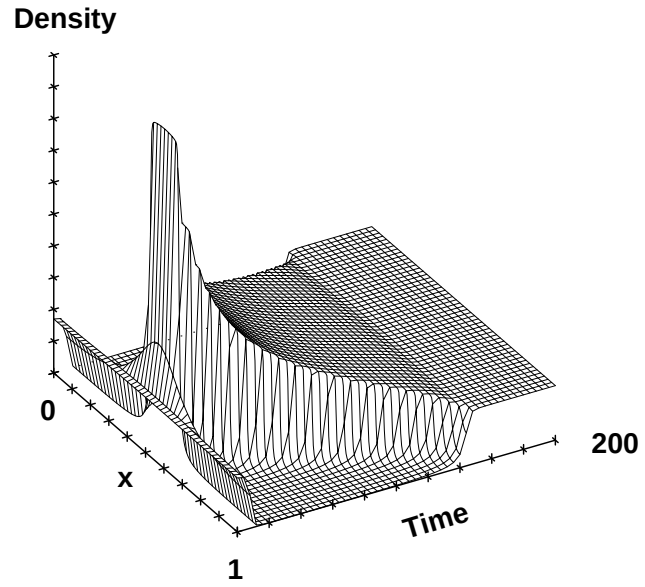

FIG. 16. *The evolution of p for the solution of* (100) *with* $\nu = 1 \times 10^{-5}$, $\beta = 0$, *and* $\mu = 0$. *Initial data are as in Figure* 14. $p_{peak}(10) = 8.22$.

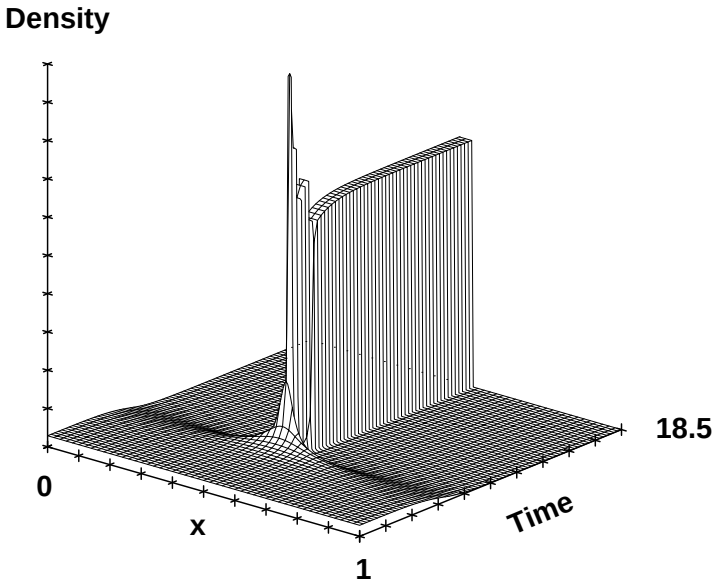

FIG. 17. *The evolution of p for the solution of* (100) *with parameters as in Figure* 15. *The initial data for p are* $2.0 - 0.01\cos(2\pi x)$ *and w is set to* $1. \times 10^{-3}$ *everywhere.* $p_{peak} = 80.7$, $p_{min}(18.5) = 1.44 \times 10^{-6}$, $p_{max}(18.5) = 44.4$.

production term that is independent of w and the solution changes quite dramatically. As is seen in Figure 19, the additional production of w leads to a much shallower and broader aggregate as compared to that shown in Figure 17.

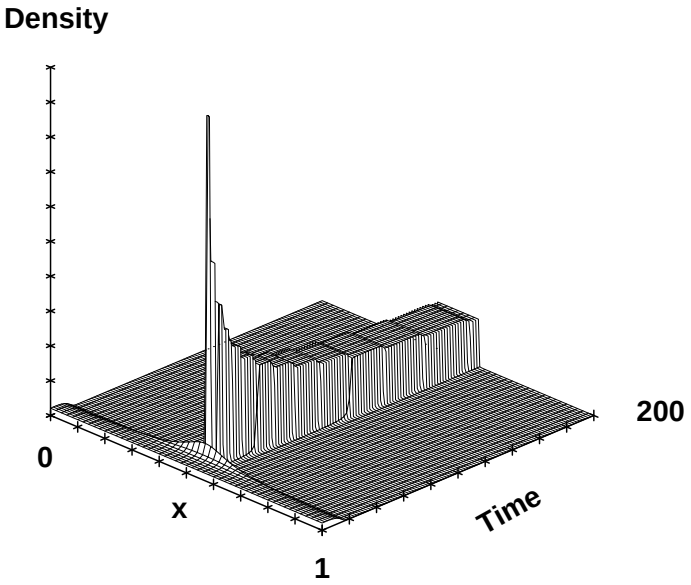

FIG. 18. *The evolution of p for the solution of* (100) *with parameters as in Figure* 15*, except that* $\mu = 0$*. The initial data for p are* $0.5 - 0.01\cos(2\pi x)$*, and w is set to* $1. \times 10^{-4}$ *everywhere.* $p_{peak} = 69.5$*,* $p_{min}(200) = 2.15 \times 10^{-6}$*,* $p_{max}(200) = 6.61$*.*

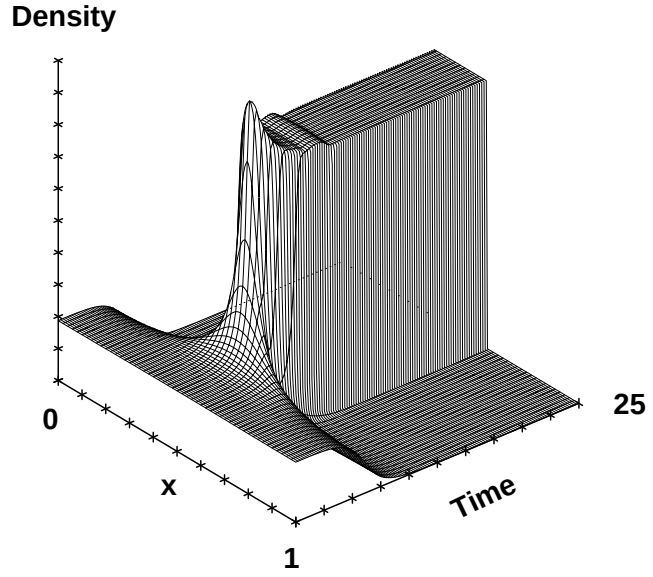

FIG. 19. *The evolution of p for the solution of* (100) *with parameters and initial data as in Figure* 17*, except* $\gamma_r = 0.1$*.* $p_{min}(25) = 1.27 \times 10^{-8}$*,* $p_{max}(25) = 8.88$*,* $p_{peak} = 10.74$*.*

6. Discussion. In this paper we derived and analyzed partial differential equations that approximate several different reinforced jump processes. One objective was to understand the qualitative behavior of the continuous equations in order to obtain a better understanding of how parameters in the microscopic movement rules translate into macroscopic parameters in the partial differential equations. We were

also interested in the correspondence between the asymptotic behavior of solutions of the partial differential equations and Davis's [3] results for the reinforced random walk that they approximate. We showed that one can obtain finite-time blowup for superlinear growth of the modulator, and collapse if it grows only linearly, starting from a single peak in the distribution of p. Strictly speaking, this is a result only for the probability density of the location of one particle or for the limiting equations of moderately interacting particles. When simulating the discrete many-particle jump process where only local interactions between the particles take place, the tactic sensitivity has to be higher to achieve aggregation, as was seen in the simplified cellular automaton model. Even exponential growth of the modulator is not sufficient in this case.

A major conclusion of our work is that within the framework of the partial differential equation models, stable aggregation can occur with local modulation of the transition rates, that is, without long range signaling via a diffusible chemical. In the context of myxobacterial aggregation this implies that trail following alone may suffice to produce aggregation if the bacteria produce a large amount of slime, at least for a short time. However, one has to keep in mind that these equations are for walkers which do not interact directly but only indirectly via w and, in particular, the kind of contact interaction that is observed experimentally is not included in the model. To date there is no model with strictly local interaction of the particles in this context, apart from the simulation model. As we have seen, in the absence of diffusion of the control species the asymptotic behavior of the bacterial density depends very strongly on the history of the process and, in particular, on the initial data, which is quite reasonable for the biological phenomenon. This is in contrast to the behavior when the modulator diffuses and stable aggregation is possible, for then there is usually an attractor for a large set of initial data and the final spatial distribution does not depend on the initial data.

We have also seen that the interplay between the production of the modulator and the chemotactic response produces a variety of interesting dynamics. At present there is little rigorous theoretical understanding of the phenomena we have described, and more work is needed on this aspect. For instance, one question of interest is whether a smooth aggregate is achievable without blowup of w. An interesting approach to a heuristic understanding of some of these phenomena is given by Levine and Sleeman [14].

Finally we shall discuss results related to those obtained here. Rascle and Ziti [24] analyzed the system

$$\begin{aligned} u_t &= \mu\Delta u - \nabla\cdot(u\chi(v)\nabla v)\,, \\ v_t &= -k(v)u\ , \end{aligned} \tag{105}$$

where $\chi(v) = \delta v^{-\alpha}$ and $k(v) = kv^m$, $\delta, k > 0$. Assuming $m < \alpha = 1$, they constructed self-similar solutions. In the case $\mu = 0$ in one space dimension, the bacterial density concentrates in the center after a finite time. In two space dimensions and initial data with $u = 0$ at the origin, one gets chemotactic rings concentrating at the origin after finite time. For higher space dimensions and an initial singularity of v at the origin, one can achieve blowup. For the case $\mu > 0$ and smooth positive initial data u blows up in finite time. But for space dimension ≥ 2 the authors were unable to construct such self-similar solutions satisfying reasonable initial conditions. This system is quite different from ours since in (105) the chemotactic species is consumed by the bacteria, whereas it is produced in our model.

There have been many studies of chemotaxis equations in which the chemotactic species is diffusible. Najundiah [19] was apparently the first to suggest that aggregation could be viewed as the development of a singularity. This viewpoint was developed by Childress and Percus [2], and there have been many studies of these equations since then [25], [15], [11]. In more recent work Mimura and coworkers incorporate growth of the "walkers" as well [17], [16].

Schaaf [25] analyzed the stationary system

$$\begin{aligned} 0 &= \nabla \cdot (\delta\ \nabla u - b(u,v)\nabla v), \\ 0 &= c\Delta v + \kappa u - \frac{\alpha v}{1+\beta v}, \end{aligned} \tag{106}$$

with Neumann boundary conditions and two forms of $b(u,v)$, viz.,

$$\begin{aligned} &\text{(a)} \quad b(u,v) = \chi u \quad \text{or} \\ &\text{(b)} \quad b(u,v) = \chi\ \frac{u}{v}. \end{aligned} \tag{107}$$

This system can be reduced to a scalar elliptic equation, and if one defines $\gamma = \frac{\chi}{\delta}$, the bifurcation results for case (b) can be summarized as follows. There exists a threshold for the cell density above which no spatially homogeneous stationary solution exists. This threshold depends on the production and decay of the chemical substance. The existence of time independent spatial structure depends on $\frac{\alpha\gamma^2}{4c}$ and $\frac{\alpha}{c}(\gamma-1)$ for $\gamma \geq 2$. The smaller c and δ are or the larger χ and α are, the more structure is possible, and the geometry of the stationary solution depends heavily on γ.

Rigorous results on the evolution problem have also been obtained recently, beginning with Jäger and Luckhaus [11], who consider the system

$$\begin{aligned} u_t &= \Delta u - \chi\nabla\cdot(u\nabla v), \\ v_t &= c\Delta v + c\kappa u - \alpha v, \end{aligned} \tag{108}$$

where $x \in \Omega \subset \mathbb{R}^N$, $u(x,0) = u_0(x), v(x,0) = v_0(x)$, and u and v fulfill Neumann boundary conditions. One rescales the variables as follows:

$$u(x,t) \to \frac{u(x,t)}{\bar{u}_0}, \quad v(x,t) \to \frac{v(x,t) - \bar{v}(t)}{\kappa\bar{u}_0}, \quad \chi \to \chi\kappa\bar{u}_0,$$

where $\bar{w}$ denotes $\frac{1}{|\Omega|}\int_\Omega w dx$. Then the rescaled system reads

$$\begin{aligned} u_t &= \Delta u - \chi\nabla\cdot(u\nabla v), \\ \epsilon v_t &= \Delta v + (u-1), \end{aligned} \tag{109}$$

where $\epsilon = \frac{1+\alpha}{c}$. Assuming that c is very large so that the equation for v is considered to be $0 = \Delta v + (u-1)$, Jäger and Luckhaus [11] prove that in two space dimensions radially symmetric solutions can blow up for suitable initial data. Nagai [18] showed that blowup cannot occur if $N = 1$, or if $N = 2$ and Ω is a ball, $v_0(x)$ is radially symmetric and $\frac{1}{|\Omega|}\int_\Omega u_0(x)dx < \frac{8}{\chi}$. Blowup occurs if this term is $> \frac{8}{\chi}$ or $N \geq 3$.

Herrero and Velázquez [8], [9], [10] first considered the same v-equation as Nagai and showed that if Ω is an open ball in $\mathbb{R}^2$ with radius R, and $T > 0$ is given, then one can obtain radial solutions $(u(r,t), v(r,t))$ such that $u(r,t)$ blows up exactly at $r = 0$, $t = T$ in such a way that $u(r,T) = \frac{8\pi}{\chi}\delta(r) + f(r)$ as $r \to 0$. The same is true for system (109) with $\epsilon > 0$.

REFERENCES

[1] D. G. Aronson, *The role of diffusion in mathematical population biology: Skellam revisited*, in Mathematics in Biology and Medicine, V. Capasso, E. Grosso, and S. L. Paveri-Fontana, eds., Springer-Verlag, New York, 1985, pp. 2–6.

[2] S. Childress and J. K. Percus, *Nonlinear aspects of chemotaxis*, Math. Biosci., 56 (1981), pp. 217–237.

[3] B. Davis, *Reinforced random walks*, Probab. Theory Related Fields, 84 (1990), pp. 203–229.

[4] M. Dworkin and D. Kaiser, *Myxobacteria* II, American Society for Microbiology, 1993.

[5] M. S. P. Eastham, *The Asymptotic Solution of Linear Differential Systems*, Clarendon Press, Oxford, 1989.

[6] P. C. Fife, *Mathematical Aspects of Reacting and Diffusing Systems*, Lecture Notes in Biomath. 28, Springer-Verlag, New York, 1979.

[7] P. Hartman and A. Wintner, *Asymptotic integration of linear differential equations*, Amer. J. Math., 77 (1955), pp. 45–86.

[8] M. Herrero and J. Velázquez, *Chemotactic collapse for the Keller-Segel model*, J. Math. Biol., to appear.

[9] M. Herrero and J. Velázquez, *Singularity patterns in a chemotaxis model*, Math. Ann., 306 (1996), pp. 583–623.

[10] M. Herrero and J. Velázquez, *A Mechanism of Blowup for the Keller-Segel Model of Chemotaxis*, preprint, 1995.

[11] W. Jäger and S. Luckhaus, *On explosions of solutions to a system of partial differential equations modelling chemotaxis*, Trans. Amer. Math. Soc., 329 (1992), pp. 819–824.

[12] N. G. V. Kampen, *Stochastic Processes in Physics and Chemistry*, North-Holland, Oxford, 1981.

[13] I. R. Lapidus, *"Pseudochemotaxis" by micro-organisms in an attractant gradient*, J. Theor. Biol., 86 (1980), pp. 91–103.

[14] H. A. Levine and B. D. Sleeman, *A system of reaction diffusion equations arising in the theory of reinforced random walks*, SIAM J. Appl. Math., 57 (1997), pp. 683–730.

[15] C.-S. Lin, W.-M. Ni, and I. Takagi, *Large amplitude stationary solutions to a chemotaxis system*, J. Differential Equations, 72 (1988), pp. 1–27.

[16] M. Mimura and T. Tsujikawa, *Aggregating pattern dynamics in a chemotaxis model including growth*, preprint, 1995.

[17] M. Mimura, T. Tsujikawa, R. Kobayashi, and D. Ueyama, *Dynamics of aggregating patterns in a chemotaxis-diffusion-growth model equation*, Forma, 8 (1993), pp. 179–195.

[18] T. Nagai, *Blow-up of radially symmetric solutions to a chemotaxis system*, Adv. Math. Sci. Appl., 5 (1995), pp. 581–601.

[19] V. Nanjundiah, *Chemotaxis, signal relaying and aggregation morphology*, J. Theor. Biol., 42 (1973), pp. 63–105.

[20] K. Oelschläger, *A fluctuation theorem for moderately interacting diffusion processes*, Probab. Theory Related Fields, 74 (1987), pp. 591–616.

[21] A. Okubo, *Diffusion and Ecological Problems: Mathematical Models*, Springer-Verlag, New York, 1980.

[22] H. G. Othmer, S. R. Dunbar, and W. Alt, *Models of dispersal in biological systems.*, J. Math. Biol., 26 (1988), pp. 263–298.

[23] C. S. Patlak, *Random walk with persistence and external bias*, Bull. of Math. Biophys., 15 (1953), pp. 311–338.

[24] M. Rascle and C. Ziti, *Finite time blow-up in some models of chemotaxis*, J. Math. Biol., 33 (1995), pp. 388–414.

[25] R. Schaaf, *Stationary solutions of chemotaxis equations*, Trans. Amer. Math. Soc., 292 (1985), pp. 531–556.

[26] H. Spohn, *Large Scale Dynamics of Interacting Particles*, Springer-Verlag, Heidelberg, 1991.

[27] A. Stevens, *A model for gliding and aggregation of myxobacteria*, in Proc. Conf. on Nonlinear Wave Processes in Excitable Media, A. Holden, M. Markus, and H. G. Othmer, eds., Plenum Press, New York, 1991, pp. 269–276.

[28] A. Stevens, *Mathematical Modeling and Simulations of the Aggregation of Myxobacteria. Chemotaxis-Equations as Limit Dynamics of Moderately Interacting Stochastic Processes*, Ph.D. thesis, Institut für Angewandte Mathematik, Universität Heidelberg, 1992.

[29] A. Stevens, *Trail following and aggregation of myxobacteria*, J. Biol. Sys., 3 (1995), pp. 1059–1068.